Solitons and solitary waves in hierarchical Korteweg-de Vries type systems

LAURI ILISON

TALLINN UNIVERSITY OF TECHNOLOGY
Faculty of Science
Department of Mechanics
Institute of Cybernetics

Dissertation was accepted for the defence of the degree of Doctor of Philosophy in Natural and Exact Sciences on April 24, 2009

Supervisor: Professor Andrus Salupere, Department of Mechanics, Institute of Cybernetics at Tallinn University of Technology

Opponents: Professor Alexey V. Porubov, A.F. Ioffe Physical Technical Institute of the Russian Academy of Sciences, St. Petersburg, Russia

Professor Henrik Kalisch, University of Bergen, Department of Mathematics, Bergen, Norway

Defence of the thesis: June 15, 2009

Declaration:
Hereby I declare that this doctoral thesis, my original investigation and achievement, submitted for the doctoral degree at Tallinn University of Technology has not been submitted for any academic degree.

/ Lauri Ilison /

Solitonid ja üksiklained hierarhilistes Kortewegi-de Vriesi tüüpi süsteemides

LAURI ILISON

Contents

List of Tables

List of Figures

10

Introduction

In our everyday world, matter is usually classified into solids, liquids and gases. What about dry sand? One grain of sand is of course a solid, but a whole lot of grains together are a granular material, with quite different properties. It flows in an hourglass. It takes the shape of its container as liquids do. If sand is poured slowly onto a surface, the pile will grow until its slope reaches a critical angle, determined by the size and stickiness of the grains. Beyond the critical angle, there is some sort of avalanche.

Hourglasses are said to have been invented at Alexandria approximately in the middle of the third century, where they were sometimes carried around as people carry watches today. First recorded evidence of the existence of hourglass was found in the 14th century for measuring the speed of ships.

Nowadays, granular materials play an important role in many of industries, such as mining, agriculture, civil engineering and pharmaceutical manufacturing. They clearly are also important for geological processes where landslides and erosion and, on a larger scale, plate tectonics determine much of the morphology of the Earth. Practically everything that we eat started out in a granular form.

The science of granular media has a long history. Much of the engineering literature has been devoted to understanding how to deal with these materials. In the literature, there are many notable names such as Coulomb who proposed the ideas of static friction, Faraday who discovered the convective instability in a vibrated container filled with powder, and Reynolds who introduced the notion of dilatancy. Moreover, today increased interest is shown in granular matter, such as particle segregation, clustering, fluidization, rotating flows, mixing and segregation, avalanches of sand piles, earthquakes, and many other interesting problems related to granular matter. The strong interest is obvious as according to Wikipedia granular materials are the second-most manipulated material in the industry (the first one is water).

Another remarkable phenomenon is related to the emergence of solitons in solids and fluids. Soliton is a solitary wave with finite energy and the necessary conditions of its existence including nonlinearity and dispersion. The dynamics of solitons is important due to their applications in hydrodynamics, electronics, solid mechanics, biophysics, and other disciplines.

In order to simulate the wave propagation in granular materials appropriate model equation shall be proposed. Historically the first continuum model for granular materials was proposed by Goodman and Cowin [5], followed by different authors.

In this thesis, the model equation proposed by Giovine and Oliveri [6] has been explored in order to simulate propagation and interactions of solitons or solitary waves in dilatant granular media. The pseudospectral method has been used for numerical integration.

This thesis is organised as follows: Section 1 introduces the solitons and their historical background in brief; describes the discovery of solitons by the Scottish

engineer James Scott Russel and presents different definitions of solitons by different authors: Russel, Zabusky and Kruskal, and Drazin. The relationship between nonlinearity and dispersion is discussed. Section 2 opens the essence of granular materials and one of the most important property of such materials — dilatancy. Section 2 also defines the theoretical basis of wave propagation in dilatant granular materials with the derivation of model equation, followed by the dispersion analysis. At the end of the Section, the statement of the problem is presented. Section 3 defines the basis of the numerical integration method and accuracy and stability controls for its results. Sections 4 and 5 analyse the emergence and interaction of solitons and solitary waves based on the numerical simulations generated by the author.

The present thesis is based on five academic papers, which are referred to in the text as "**Publication I**", "**Publication II**", "**Publication III**", "**Publication IV**", "**Publication V**":

Publication I	**Lauri Ilison**, Andrus Salupere and Pearu Peterson, *On the propagation of localized perturbations in media with microstructure*, Proc. Estonian Acad. Sci. Phys. Math., 2007, 56, 2, 84–92.
Publication II	Andrus Salupere, **Lauri Ilison**, and Kert Tamm. *On numerical simulation of propagation of solitons in microstructured media*, In Michail D. Todorov, editor, Proceedings of the 34th Conference on Applications of Mathematics in Engineering and Economics (AMEE 2008), volume 1067 of AIP Conference Proceedings, 155–165. American Institute of Physics, 2008.
Publication III	**Lauri Ilison** and Andrus Salupere, *Propagation of* sech^2- *type solitary waves in hierarchical KdV-type systems*, Mathematics and Computers in Simulation, 22 pp., Elsevier, 2009. (accepted).
Publication IV	Andrus Salupere and **Lauri Ilison**, *Numerical simulation of interaction of solitons and solitary waves in granular materials*, In J.F. Ganghoffer and Franco Pastrone, editors, Proceedings of EUROMECH - MECAMAT conference, Mechanics in microstructured solids: cellular materials, fibre reinforced solids and soft tissues, Lecture Notes in Applied and Computational Mechanics, 8 pp., Springer, 2009. (accepted).
Publication V	**Lauri Ilison** and Andrus Salupere, *Numerical simulation of interaction of solitons and solitary waves in hierarchical KdV-type systems*, Communications in Nonlinear Science and Numerical Simulations, 10 pp., Elsevier, 2009. (submitted).

Detailed descriptions of the numerical results are presented in two research reports, which are referred to in the text as "**Report I**" and "**Report II**":

Report I   **Lauri Ilison**, Andrus Salupere. *Propagation of localised perturbations in granular materials.* Research Report Mech 287/07, Institute of Cybernetics at Tallinn University of Technology, 2007.

Report II   **Lauri Ilison**, Andrus Salupere. *Interactions of solitary waves in hierarchical KdV-type system.* Research Report Mech 291/08, Institute of Cybernetics at Tallinn University of Technology, 2008.

Approbation

The results of the thesis have been presented at the following conferences:

1. Andrus Salupere, Jüri Engelbrecht, **Lauri Ilison**, and Kert Tamm. *On Solitary Waves and Solitons in Hierarchical Systems.* IMACS 2005, The Forth International Conference on Nonlinear Evolution Equations and Wave Phenomena: Computation and Theory, 10–14 April, 2005, The University of Georgia, Athens, USA.

2. Andrus Salupere, Jüri Engelbrecht, Olari Ilison, and **Lauri Ilison**. *Propagation of Solitary Waves in Microstructured Media.* FUDoM 2005, Finno-Ugric International Conference of Mechanics with ESI Group Symposium, 29 May–4 June, 2005, Ráckeve (Budapest), Hungary.

3. Andrus Salupere, Jüri Engelbrecht, Olari Ilison, and **Lauri Ilison**. *Solitary Waves Governed by Complicated Nonlinearity and Dispersion.* FPU+50: Nonlinear Waves 50 Years After Fermi-Pasta-Ulam. 21–25 June, 2005, INSA de Rouen, France.

4. Andrus Salupere, Jüri Engelbrecht, Olari Ilison, and **Lauri Ilison**. *On Solitary Waves and Solitons in Microstructured Media.* RANM 2005, Recent Advances in Nonlinear Mechanics, 30 Aug–1 Sept, 2005, University of Aberdeen, Scotland, UK.

5. **Lauri Ilison** and Andrus Salupere. *On the propagation of localised perturbations in continua with microstructure.* EUROMECH Colloquium 478, Non-equilibrium Dynamical Phenomena in Inhomogeneous Solids, 13–16 June, 2006, Tallinn, Estonia.

6. **Lauri Ilison** and Andrus Salupere. *On the formation and interaction of solitons and solitary waves in granular media.* Dynamics Days Europe 2007, Loughborough University, UK, 9–13 July, 2007.

7. Andrus Salupere and **Lauri Ilison**. *Numerical simulation of interaction of solitons and solitary waves in granular materials.* 11th EUROMECH - MECA-MAT Conference "Mechanics of microstructured solids: cellular materials, fibre reinforced solids and soft tissues", Torino, Italy, 10–14 March, 2008.

8. **Lauri Ilison** and Andrus Salupere. *Solitons and solitary waves in granular materials.* 11th Estonian Days of Mechanics, 15–16. Sept., 2008, Tallinn, Estonia.

9. Andrus Salupere and **Lauri Ilison**. *On interaction of solitary waves in granular materials.* 7th EUROMECH Solid Mechanics Conference (ESMC2009), Lisbon, Portugal, 7–11. Sept., 2009. (accepted).

Acknowledgments

1 Solitons and solitary waves

1.1 History of solitons and Korteweg–de Vries type equations

Historically, the first documented observation of a soliton was made by a Scottish engineer John Scott Russel in August 1834 when he saw a rounded smooth well-defined heap of water detach itself from the prow of a barge brought to rest and proceed without change of shape or diminution of speed for over two miles along the Union Canal linking Edinburgh with Glasgow. John Scott Russell described his *wave of translation* in his own words: *"I was observing the motion of a boat which was rapidly drawn along a narrow channel by a pair of horses, when the boat suddenly stopped — not so the mass of water in the channel which it had put in motion; it accumulated round the prow of the vessel in a state of violent agitation, then suddenly leaving it behind, rolled forward with great velocity, assuming the form of a large solitary elevation, a rounded, smooth and well-defined heap of water, which continued its course along the channel apparently without change of form or diminution of speed. I followed it on horseback, and overtook it still rolling on at a rate of some eight or nine miles an hour, preserving its original figure some thirty feet long and a foot to a foot and a half in height. Its height gradually diminished, and after a chase of one or two miles I lost it in the winding's of the channel. Such, in the month of August 1834, was my first chance interview with that singular and beautiful phenomenon which I have called the Wave of Translation"* [7].

His observations were followed by extensive practical and theoretical experiments of these waves. He built wave tanks at his home and noticed important properties of those waves [8]:

- These localised waves are bell-shaped and travel with permanent form and velocity.

- In water of undisturbed depth, h a wave of elevation a_m, towards which the crest points, propagates with a velocity $v = \sqrt{g(h + a_m)}$, where g is the gravity.

- An initial elevation of water might, depending on the relation between its height and length, evolve into a pure solitary wave, a single solitary wave plus a residual wave train, or two or more solitary waves with or without residual wave train.

- The solitary waves can across each other without a change of any kind.

- Solitary waves of depression are not observed: an initial depression is transformed into an oscillatory wave train of gradually increasing length and decreasing amplitude.

Independently, Joseph Boussinesq (1871) and Lord Rayleigh (1876) added important findings: if one ignores dissipation, the increase in local wave velocity associated with the finite amplitude is balanced by the decrease associated with dispersion, leading to a wave of a permanent form [8, 9]. In 1895, Korteweg and de

Vries derived a model equation which describes the unidirectional propagation of long waves in the water of relatively shallow depth. This equation has become much celebrated and it is now known as the Korteweg–de Vries (KdV) equation. Korteweg and de Vries showed that periodic solutions, which they named cnoidal waves, could be found in close form and without further approximations. Moreover, they found a localised solution, which represents a single hump of positive elevation and occurs in the limit of the finite wavelength or the spatial period of the cnoidal wave. This hump is the solitary wave discovered experimentally by Russell [7, 8, 10, 11, 1].

1.2   Definition of solitons

In the course of time different authors have given different definitions of solitons. Remoissenet [8] brings to light three concepts. The first definition is related to the first documented observation of a solitary water wave by John Scott Russell:

- A solitary wave, as discovered by Russell [7], is a localised wave that propagates along one space direction only, with an undeformed shape.

The second definition is quite mathematical and is related to integrable systems, i.e., to idealised conditions:

- A soliton, as discovered numerically by Zabusky and Kruskal [2], is a large amplitude coherent pulse or a very stable solitary wave, the exact solution of a nonlinear wave equation, whose shape and speed are not altered by a collision with other solitary waves.

For physicists who study the real world, the keyword soliton has a weaker meaning. They present the definition which highlights the importance of a particular type of energy propagation as follows:

- Solitons are localised finite energy states which are fundamentally nonlinear objects and so cannot be reached by the perturbation theory from any linear state.

The present study uses the soliton concept given by Drazin [10, 11] and Zabusky [12].

According to Drazin [10, 11]:

- The term soliton is associated with any solution of a nonlinear equation or system which (i) represents a wave of permanent form; (ii) is localised so that it decays or approaches a constant at infinity; (iii) can interact strongly with other solitons and retain its identity.

According to Zabusky [12]:

- A soliton is defined as a localised or solitary entity that propagates at a uniform speed and preserves its structure (or shape) and speed in an interaction with another such solitary entity.

Therefore, a solitary wave can be called a soliton if it propagates at constant speed and shape and restores its speed and shape after interactions. Interactions of such a type are commonly called elastic interactions.

Historically [1], Zabusky and Kruskal have coined the word *soliton*, which they introduced by putting it, for the first time, in the title of their paper [2]. In order to stress the quasi-particle properties of the solitary waves they thought of the suffix *'on'*, as in electron, proton, boson etc. Zabusky first proposed *solit-r-on* as an abbreviation of a *solita-r-y wave* before noticing that it was the name of a company in the United States. They finally opted for *soliton*, which is now in common use [1].

1.3 Solitons in the Nature

In the Nature the phenomena of solitons have been discovered in many fields: (i) solitons in shallow water, (ii) solitons in fibre optics, (iii) solitons in composite materials, (iv) solitons in plasma, (v) atmospheric solitons, (vi) solitons in neuroscience, (vii) solitons in magnets and in many other fields [1, 13].

Solitons are surrounding us and we need to be patient to find them. As a proof of that, during my short trip to the resort of Kauksi on Lake Peipsi in Estonia on 17th of July 2003 I was observing how solitons emerged and interacted in very shallow water. Soomere and Engelbrecht have described this as an example of Kadomtsev–Petviashvili solitons in shallow water [14, 15, 16].

The solitons are generated due to beach profile and appropriate weather conditions. There had been an avalanche of sand from the beach to the water, causing a bell–shape submerged cape bottom profile. The measures of this cape where

Figure 1: Interaction patterns of soliton-like surface waves in very shallow water near the Kauksi resort on Lake Peipsi, Estonia (Photo taken by the author, July 2003)

approximately 8–metre long perpendicular to the beach and 5–metre wide. The depth of the shallow water was approximately 3 to 10 cm. The wind was very low,

as it can be seen from the picture, see Fig. 1. Wind waves propagated nearly perpendicular to the beach and the bell–shape cape bottom turned the wind wave propagation direction around it from the left and the right hand side of the cape. As a result (see Figs. 1 and 2) — (i) solitons in shallow water emerged, (ii) solitons emerged from both sides of the bell–shape bottom profile at the right angle, (iii) solitons interacted elastically. Those pictures will be published by Soomere in [17].

Figure 2: Interaction patterns of soliton-like surface waves in very shallow water near the Kauksi resort on Lake Peipsi, Estonia (Photo taken by the author, July 2003)

1.4 Korteweg–de Vries equation

For future discussions, nature of the Korteweg–de Vries (KdV) equation must be explained. One of the widely used forms of the KdV equation is

$$u_t + u\,u_x + d\,u_{3x} = 0, \tag{1}$$

where u is the excitation, t and x are time and space coordinates, respectively, d stands for the dispersion parameter. Different properties of the KdV equation are discussed in detail in [18].

One could emphasise two important facts involved in the KdV equation:

- the KdV equation was used to introduce the soliton concept;

- for solitons to exist, the dispersive and nonlinear properties of the media should be in a certain balance.

The KdV equation involves the corresponding terms ($u\,u_x$ for nonlinearity and $d\,u_{3x}$ for dispersion) in the simplest form.

As the celebrated KdV equation (1) is an integrable equation [18], its stationary solution in a frame moving with a velocity c can be found analytically. If we substitute

$$u(x,t) = u(\xi), \tag{2}$$

where $\xi = x - ct$ into Eq. (1), then for u we obtain a third-order nonlinear ordinary differential equation (ODE)

$$-cu_\xi + u u_\xi + d u_{3\xi} = 0. \tag{3}$$

Here c is the phase velocity. The solution of ODE (3) can be found directly by integrating the differential equation for three times.

In the case of asymptotic boundary conditions

$$u, u_\xi, ..., u_{3\xi} \longrightarrow 0, \text{ if } \xi \longrightarrow \pm\infty \tag{4}$$

the solution can be expressed in the following form:

$$u = 3c \operatorname{sech}^2 0.5\sqrt{\frac{c}{d}}(\xi - \xi_0) = A \operatorname{sech}^2 \sqrt{\frac{A}{12d}}(\xi - \xi_0), \tag{5}$$

where ξ_0 is an arbitrary constant [2]. The behaviour of the solitary wave solution (5) corresponds to the soliton definition: such solitary waves propagate with constant speed and shape and the interaction of such solitary waves is elastic. Here the quantity $A = 3c$ can be considered as the amplitude of the soliton, i.e., the higher the soliton, the higher its velocity. An example of a typical soliton emergence is given in Fig. 3, where the initial excitation is decomposed into three solitons which have elastic interactions.
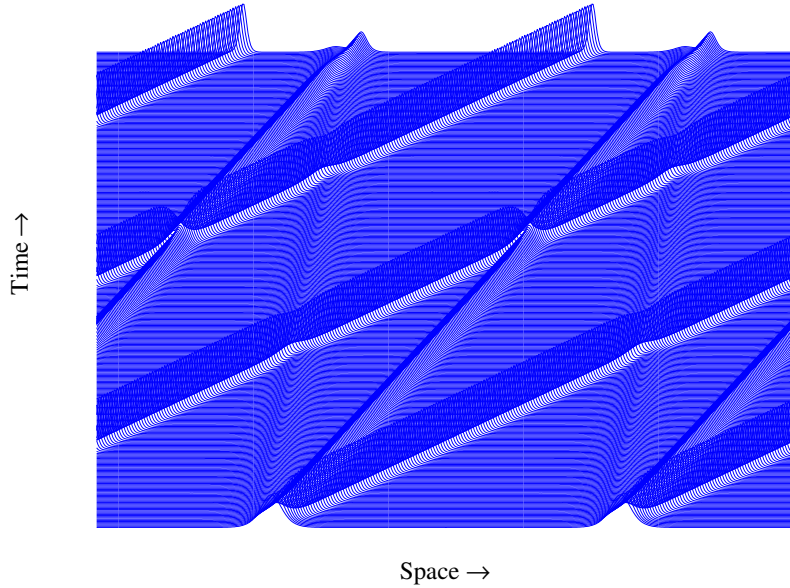
Figure 3: Emergence of a train of three KdV solitons and subsequent elastic interactions. Calculated by Salupere

1.5 Higher order KdV equations

During recent years KdV-type equations with higher-order dispersive and/or non-linear terms have been studied by many authors. It is obvious that the original KdV equation is obtained at a certain degree of approximation (higher-order dispersive or nonlinear effects have been neglected), but in many cases the physical reality needs better accuracy and the higher-order effects should be taken into account.

As an example, in the case of water waves where the surface tension suppresses the dispersion parameter d, the fifth-order dispersion u_{5x} is added by Hunter and Scheurle [19]

$$u_t + u u_x + d u_{3x} + u_{5x} = 0. \tag{6}$$

Furthermore, the third-order dispersive term may be so weak, for example, as defined by Kakutani and Ono [20] for the magneto-acoustic wave propagation in a cold collision-free plasma, that it vanishes and is replaced by the fifth-order dispersive term resulting in a fifth-order KdV equation

$$u_t + u u_x + u_{5x} = 0. \tag{7}$$

Karpman and Vanden-Broeck [21] have shown numerically that the fifth-order derivative term of the equation

$$u_t + \alpha u^p u_x + \beta u_{3x} + \gamma u_{5x} = 0, \tag{8}$$

is of critical importance for the soliton stability at sufficiently high values of p.

Kawamoto [22] has considered the KdV equation with higher-order nonlinearity

$$u_t + (\alpha u^3 + \beta u^2 + \gamma u)x_x + \delta u_{3x} = 0, \tag{9}$$

as a model for the wave propagation in a one-dimensional nonlinear lattice of nonlinear LC network, where α, β, γ and δ are arbitrary constants.

Porubov et al. [23, 24] have studied the influence of higher-order nonlinear terms on the shape of solitary waves for mechanical systems governed by an extended KdV equation — a generalisation of the fifth-order KdV equation

$$u_t + 2b u u_x + 3c u^2 u_x + r u u_{3x} + s u_x u_{2x} + d u_{3x} + f u_{5x} = 0, \tag{10}$$

where b, c, r, s, d and f are appropriate coefficients for a certain case.

O. Ilison and Salupere [25, 26] and Salupere et al. [27] have studied the KdV–like equation

$$u_t + [P(u)]_x + d u_{3x} + b u_{5x} = 0, \tag{11}$$

where d and b are the third- and fifth-order dispersion parameters, respectively, and the fourth-order elastic potential

$$P(u) = \left(-\frac{u^2}{2} + \frac{u^4}{4} \right) \tag{12}$$

21

depicts the quartic nonlinearity in the simplest symmetrical form. Equation (11) with potential (12) describes the wave propagation in shape memory alloys where the higher-order dispersion is caused by the crystal structure.

Marchant applied a modified KdV equation for modelling the behaviour of undular bores and derived two analytical undular bore solutions for the initial-value problem [28].

Soomere et al. [14] studied two-soliton solutions of the Kadomtsev-Petviashvili (KP) equation with unequal amplitudes with the use of the concept of the interaction soliton (introduced by Peterson and van Groesen in [29]). The standard KP equation in normalised variables (u, x, y, t) reads

$$\left(u_t + 6u\,u_x + u_{3x}\right)_x + 3u_{yy} = 0, \tag{13}$$

where $\eta = (x, y, t)$ describes a certain disturbance, e.g., the elevation of the water surface.

Tan et al. studied the evolution of perturbed embedded solitons in the general Hamiltonian fifth-order KdV equation [30]

$$u_t + u_{3x} + u_{5x} + \left\{N(u)\right\}x = 0, \tag{14}$$

where the nonlinear term $N(u)$ is of the form $N(u) = \alpha_0 u^2 + \alpha_1 u\,u_{2x} + \alpha_2 u_x^2 + \alpha_3 u^3$.

Ludu [31] has used a polynomial differential equation of the KdV type to investigate the soliton-antisoliton transition. Ludu and Kevrekidis examined how nonlinear dispersion relations can be used as a simple, universal algebraic tool to provide information for the localised, nonlinear solutions of PDE that model physical systems. Among presented examples, KdV, modified KdV and $K(m, n)$ equations were considered [32].

Gou and Taha [33] worked out parallel algorithms for the split-step Fourier transform and the pseudospectral methods in order to investigate self-focusing singularity problem in the case of a higher-order KdV equation.

Pelinovsky and Sergeeva studied numerically the evolution of the initially random wave field with a Gaussian spectrum shape within the KdV equation [34].

1.6 Nonlinearity and dispersion

The KdV equation (1) appears in many areas of physics, where waves emerge in a weakly nonlinear and dispersive medium. The essence of nonlinearity and dispersion is explained (see [1]) to provide a better understanding of those important properties.

Let us consider Eq. (1) without the dispersive term

$$u_t + u\,u_x = 0, \tag{15}$$

which is called the Burgers–Hopf equation. The coefficient of u_x determines the propagation speed of the wave, so that, as a first approximation, one notices that each component of the signal moves with a speed u. As a result, the parts of the

signal which have the largest amplitude u tend to move faster than the parts which have smaller amplitudes. Fig. 4 shows that this situation favours the formation of shock waves, i.e., waves which exhibit discontinuities in a finite time, where variations of the filed have a vertical slope. This analysis is confirmed by the exact solution of the Burgers–Hopf equation (see Fig. 4). In order to explain the essence
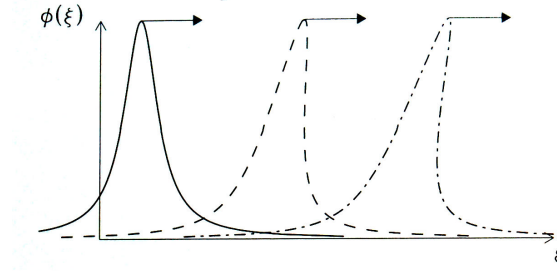
Figure 4: Time evolution of a pulse which is a solution of the Burgers–Hopf equation (15) (Dauxois and Peyrard [1])

of dispersion the linearised version of Eq. (1) is considered:

$$u_t + d\, u_{3x} = 0. \tag{16}$$

It has harmonic wave solutions of the form

$$u = A e^{i(k\xi - \omega\tau)} \tag{17}$$

provided the frequency ω and the wavenumber k are linked by the dispersion relation $\omega = -k^3$ and phase velocity $c_p = \omega/k = -k^2$, which depends on the wavenumber k. This characterises a dispersive medium, where the Fourier components of narrow pulse propagate at different speeds, which leads to a broadening of the pulse (see Fig. 5). The existence of a permanent profile soliton solu-
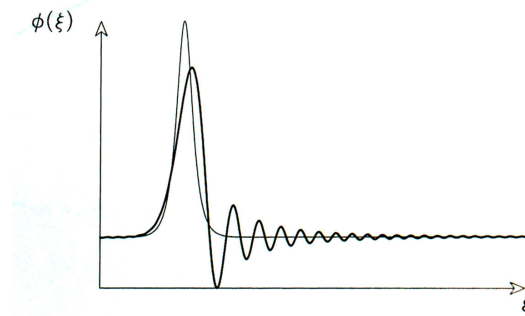
Figure 5: Time evolution of a pulse which is a solution equation (16) (Dauxois and Peyrard [1])

23

tion of the KdV equation results from a balance between the nonlinearity and dispersion: nonlinearity tends to localise and/or steepen the wave while dispersion spreads it out. This equilibrium is stable. If the initial pulse is too narrow, dispersive effects dominate and tend to broaden the pulse until equilibrium is reached. If the initial pulse is too broad, nonlinear effects dominate, which tend to localise the pulse until equilibrium is reached [1].

The first description of such a process was given by Zabusky and Kruskal [2] in 1965. Initially the first two terms of KdV equation (1) — terms of nonlinearity — dominate, u steepens in the regions where it has a negative slope, see Fig. 6. Secondly, after u has steepened sufficiently, the third term — dispersion — be-
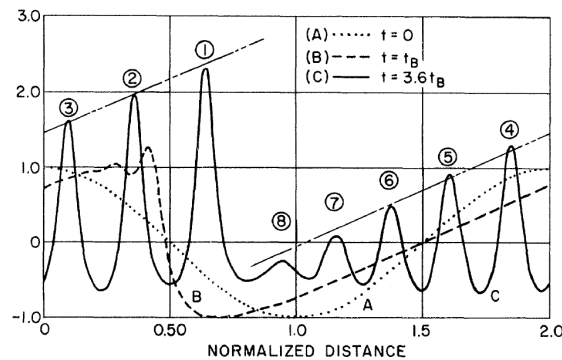
Figure 6: Temporal development of the wave form $u(x)$ (Zabusky and Kruskal [2]). Curve (A) corresponds to the time moment $t = 0$, curve (B) corresponds to the time moment $t = 1/\pi$ and curve (C) corresponds to the time moment $t = 3.6/\pi$

comes important and serves to prevent the formation of a discontinuity. Instead, oscillations of small wavelength develop on the left of the front. The amplitudes of the oscillations grow and finally each oscillation achieves almost a steady amplitude. Finally, each of such solitary-wave pulses or solitons begins to move uniformly at a rate that is linearly proportional to its amplitude. Thus, the solitons spread apart. Because of the periodicity (in terms of space periodicity), two or more solitons eventually overlap spatially and interact nonlinearly.

2 Wave propagation in dilatant granular materials

2.1 Granular materials

A granular material can be defined as a material composed of many individual solid particles irrespective of particle size, i.e., they are large conglomerations of discrete macroscopic particles. If granular materials are non-cohesive, then forces between them are essentially only repulsive so that the shape of the material is determined by external boundaries and gravity. There is, however, a particular problem with regard to density, since there are two densities of interest, the density of particles themselves, which will be called as solid density and the density of the mixture of a solid and an interstitial gas or a liquid that is known as the bulk density. Fluid-like behaviour can be found in these materials that are very much alike, similar phenomena are exhibited by conventional liquids.

Granular materials exhibit a number of distinctive features not shared by ordinary solids or fluids. In fact, depending on the externally applied mechanism they behave somewhat like solids or fluids. Furthermore, their behaviour can be in a process change form, say being fluid-like to suddenly solid-like, often repeatedly, so that an intermittent reaction results from a driving mechanism that may strictly be continuous.

2.2 Dilatancy

A unique property of a granular material was observer by Reynolds [35] who named it *dilatancy*. The concept of dilatancy is generally taken to be the expansion of the voidage that occurs in a tightly packed granular arrangement when it is subject to a deformation. Reynolds [35] used the idea of dilatancy in describing a familiar phenomenon in sand: *"At one time the sand will be so firm and hard that you may walk with high heels without leaving a footprint; while at others, although the sand is not dry, one sinks in so as to make walking painful. Had you noticed, you would have found that the sand is firm as the tide falls and becomes soft again after it has been left dry for some hours. The tide leaves the sand, though apparently dry on the surface, with all its interstices perfectly full of water which is kept up to the surface of the sand by capillary attraction; at the same time the water is percolating through the sand from the sands above where the capillary action is not sufficient to hold the water. When the foot falls on this water-saturated sand, it tends to change its shape, but it cannot do this without enlarging the interstices — without drawing in more water. This is a work of time, so that the foot is gone again before the sand has yielded."* Many of the existing theories for flowing granular materials use this observation to relate the applied stress to the voidage and the velocity. One of the first and most interesting observations of the relationship between the stress in granular materials and voidage was also given by Reynolds [36]: *"Taking a small Indian rubber bottle with a glass neck full of shot and water, so that the water stands well into the neck. If instead of the shot the bag were full of water or had anything of the nature of a sponge in it, when the bag was squeezed, the water would be forced*

up the neck. With the shot the opposite result is obtained; as I squeeze the bag, the water decidedly shrinks in the neck... (see Fig. 7) When we squeeze a sponge between two planes, water is squeezed out; when we squeeze sand, shot, or granular material, water is drawn in." The idea of dilatancy of granular materials can be simply
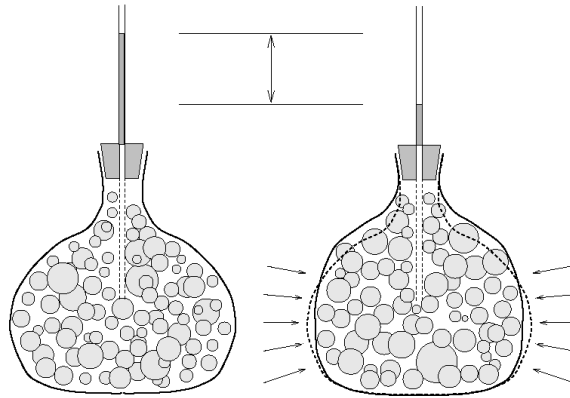
Figure 7: Rubber bellows filled with a granular material of densest packing and sealed with a plug and pore space filled with water, of which the filling is made visible by the liquid level in the pipette. Outside pressure deforms the content, also by shear; the water level in the pipette falls as a result of the pore space extension (Wand and Hutter [3])

explained for an idealised case: in order for a shearing motion to occur in a bed of closely packed spheres, the bed must expand by increasing its void volume, see Fig. 8.
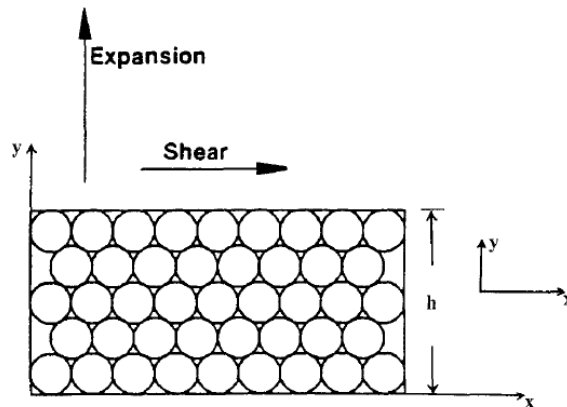
Figure 8: An illustration of dilatancy in an ensemble of initially close-packed spheres (Massoudi and Mehrabadi [4])

26

2.3 Continuum theory for granular materials

The continuum description of granular materials has attracted scientists' interest over the last fifty years. During the recent ten years many authors have published papers on the continuum description of granular materials. Godano and Oliveri [37] have proposed a possible mathematical model of site effects that occur when seismic waves propagate through a sediment fillet basin. Massoudi et al. [4] have explored the consequences of the Mohr–Coloumb criterion of the constitutive equations. The continuum model based on the work of Cowin [38] allows for predicting the dilatancy effect which is related to the normal stress effects. Fang et al. [39] have derived thermodynamically consistent continuum theory for single–phase, single–constituent cohesionless granular materials. Giovine [40] has extended the continuum theory for granular materials with freedom for particle rotations resulting in a theory that considers three terms of microstructural motions: rotation of granules, dilatational expansion and contraction of individual compressible grains and of the grains relative to other ones.

Historically, the first model for granular materials based on the formal arguments of continuum mechanics was proposed by Goodman and Cowin [5]. The basic premise underlying the model is that the concept of mass distribution must be extended to admit granular materials. The distribution of mass must be related to the volume distribution of granules. To achieve that, an independent kinematical variable — volume distribution function — was introduced. The following physically motivated assumptions associated with the volume distribution of granules in a granular material form the basis of the theory [5]:

- The volume of granules in a granular material is regarded as a measure on the Euclidean space. The measure is valid for solids, porous materials (rock, cork, sponge, etc.) as well as for granular materials (sand, grain, powder, etc.).

- The measure of mass is assumed to be continuous with respect to the measure of volume distribution. This assumption is equivalent to neglecting the void mass and is consistent with one's intuitive notion of granular materials, i.e., considering the dry sand. The science of the void mass is neglected, only one type of a material point needs to be considered to describe the motion of a body.

- To account the energy flux and energy supply associated with the time rate of volume distribution change, a higher-order stress and body force are introduced.

- From a conceptual viewpoint, the flow behaviour of granular materials is considered to be similar to the fluid behaviour. Specifically, the response of a granular material is unaltered by any change in the reference configuration that does not change the density and volume distribution. The condition on the volume distribution requires that the granular material have preferred reference configuration with respect to volume distribution.

The theory proposed by Goodman and Cowin [5] has been modified and extended by many authors, especially by Bedford and Drumheller [41].

2.4 Model equation

The flow behaviour of granular materials is considered to be similar to the fluid behaviour except that its response depends on the distribution of the volume fraction in the reference placement. Moreover, the introduction of the volume fraction of the grains as an independent kinematical variable in order to describe the local deformations of the grains themselves, requires an additional balance equation for the microinertia. The model equation presented below is derived by Giovine and Oliveri [6].

The equations of motion for the dilatant granular material are obtained from a Hamiltonian variational principle of local type in the conservative case. The propagation of nonlinear waves in a region with uniform state is studied by means of an asymptotic approach that has already appeared useful in an investigation on wave propagation in bubbly liquids and in fluid mixture. When the grains are assumed to be incompressible, then the material behaves as a continuum with a latent microstructure.

An element of the continuum is thought as a spherical envelope of radius ς containing some spherical inclusions (the grains) of radius ϑ such as the case of a suspension of elastic particles in a compressible fluid whose density is considered to be negligible compared to the proper solid density ρ_m of suspended particles; so the bulk density ρ of the body equals ρ_m times the volume fraction v of the grains

$$\rho = \rho_m v, \tag{18}$$

where the volume fraction $0 < v < 1$. Neither diffusion of the grains through the envelope, nor effects of relative rotations of the element or the grains themselves are recognised, so the only allowed motions within the element are merely expansions and contractions of the inclusions and radial motions of the spherical crust due to the displacements of the grain relative to the centre of mass of the element itself. These assumptions are rather limiting for this type of media, but necessary to obtain appropriate expression of the energy density. If v denotes the velocity of the centre of the mass of the element whose local position vector is x at the time τ, then the density per unit mass of the total kinetic energy k of the material turns out to be

$$\kappa = \frac{1}{2}v^2 + \frac{1}{2}\gamma(\rho)\dot{\rho}^2 + \frac{1}{2}\alpha(\rho_m)\dot{\rho}_m^2 \tag{19}$$

where the dot $\dot{}$ denotes the material time derivative. An explicit evaluation for the constitutive functions $\gamma(\rho)$ and $\alpha(\rho_m)$ can be made when the grains and the elements expand or contract homogeneously with independent motions. In the following model, the case described involves the suspension of the grains considered, as in a fixed rigid vessel, being very large with respect to grains and to single element of the medium. If $\mathscr{B}$ is the region of space delimited by the vessel and $\partial\mathscr{B}$

28

its boundary, then the kinematic compatibility condition requires

$$v \cdot n = 0 \text{ on } \partial \mathscr{B}, \tag{20}$$

where n is the unit exterior vector normal to $\partial \mathscr{B}$. The conservation of mass requires

$$\dot{\rho} + \rho \operatorname{div} v = 0 \text{ in } \mathscr{B}. \tag{21}$$

The dynamical equations of motion are derived from a Hamiltonian variational principle of local type in the conservative case. It is assumed that the internal actions on $\mathscr{B}$ must be derived from the potential energy density φ. Since the material is essentially thought as a perfect fluid in its behaviour, φ is assumed to be the function of the state of $\mathscr{B}$ through ρ, $\operatorname{grad} \rho$ and $\operatorname{grad} \rho_m$.

The condition (20) requires that the variation δx is tangent to the boundary $\partial \mathscr{B}$

$$\delta x \cdot n = 0 \text{ on } \partial \mathscr{B}. \tag{22}$$

Based on the condition (22) one can define the global virtual work of external actions, resulting from the virtual displacement δx and from a change $\delta \rho_m$ of the proper density of the matrix, which includes the microvariations of the microstructure of the elements, as the quantity

$$\delta \mathscr{L} = \int_{\mathscr{B}} \rho (f \cdot \delta x + \beta \hat{\delta} \rho_m) d \mathscr{B} \tag{23}$$

where $\mathscr{L}$ is Lagrangian, f and β are the densities of the unit mass of external body and microstructural forces.

The Hamiltonian principle in the local form asserts that, during the natural motion of the body the equality

$$\hat{\delta} \int_{\tau_0}^{\tau_1} d\tau \int_{\mathscr{B}} \rho(\kappa - \varphi) d \mathscr{B} + \int_{\tau_0}^{\tau_1} \delta \mathscr{L} d\tau = 0 \tag{24}$$

holds for all virtual processes. The applied operator $\hat{\delta}$ means the variation of the next integral functional defined on a variable region. $\delta \mathscr{L}$ is a global virtual work of external actions resulting from the virtual displacement δx and from a change $\delta \rho_m$, which includes the microvariations of the microstructure of the elements (see [6]).

After rigorous mathematical transformations (see [6]) and making use of the asymptotic approach (one-dimensional motion is considered), the transport equation ruling the evolution of a perturbation propagating near the region of an equilibrium of a dilatant granular material can be obtained

$$\frac{\partial u}{\partial t} + u \frac{\partial u}{\partial x} + \alpha_1 \frac{\partial^3 u}{\partial x^3} + \beta \frac{\partial^2}{\partial x^2} \left(\frac{\partial u}{\partial t} + u \frac{\partial u}{\partial x} + \alpha_2 \frac{\partial^3 u}{\partial x^3} \right) = 0, \tag{25}$$

29

where u is the density, x is the space coordinate (variable), t is the time coordinate (variable), α_1 denotes the macrostructure dispersion parameter, α_2 denotes the microstructure dispersion parameter and β can be called as the microstructure parameter involving the ratio of the grain size and the wavelength. The parameter β can be positive or negative depending on the ratio of kinetic and potential energies of the particles. For lower values of kinetic energy, the parameter β is positive and for higher values negative. The exact definitions of the parameters α_1, α_2 and β can be found in [6].

Mathematically, Eq. (25) consists of two KdV operators: the first describes the influence of the macrostructure and the second (in the brackets) - the influence of motion in the microstructure. Equation (25) is clearly hierarchical in the Witham's [42] sense — if the parameter β is small, then the influence of the microstructure can be neglected and the wave "feels" only the macrostructure. If, however, the parameter β is large, then only the influence of the microstructure "is felt" by the wave. Due to that kind of hierarchy, Eq. (25) could be called as the hierarchical Korteweg–de Vries (HKdV) equation. If the grains are assumed to be incompressible, then the material behaves as a continuum with the latent microstructure and the evolution equation describing the wave propagation takes the form of the classical KdV equation with an appropriate value for the dispersion parameter α.

$$\frac{\partial u}{\partial t} + u \frac{\partial u}{\partial x} + \alpha \frac{\partial^3 u}{\partial x^3} = 0. \tag{26}$$

The exact definitions of the parameter α can be found in [6].

2.5 Dispersion analysis

In this Section the dispersion analysis is presented for Eq. (25). For the dispersion analysis the model Eq. (25) is linearised and the dispersion relation, phase- and group velocities are derived. The character of dispersion is analysed in the space of parameters α_1, α_2 and β.

To obtain the linear dispersion relation for the evolution Eq. (25), sinusoidal wavetrain

$$u = a e^{i(kx - \omega t)} \tag{27}$$

expression that models 1D waves in dilatant granular materials is substituted in the linearised model equation

$$\frac{\partial u}{\partial t} + \alpha_1 \frac{\partial^3 u}{\partial x^3} + \beta \frac{\partial^2}{\partial x^2} \left(\frac{\partial u}{\partial t} + \alpha_2 \frac{\partial^3 u}{\partial x^3} \right) = 0. \tag{28}$$

This substitution results in the following equation:

$$-i a w e^{i(kx - \omega t)} - i \alpha_1 a k^3 e^{i(kx - \omega t)} - \tag{29}$$
$$i a \beta k^2 \omega e^{i(kx - \omega t)} - i \alpha_2 a \beta k^5 e^{i(kx - \omega t)} = 0.$$

Expressing the angular frequency ω from Eq. (29), we obtain the dispersion relation

$$\omega = \frac{\alpha_1 k^3 - \alpha_2 \beta k^5}{\beta k^2 - 1}. \tag{30}$$

From the latter, the phase velocity

$$c_p = \frac{(\alpha_1 - \alpha_2 \beta k^2) k^2}{\beta k^2 - 1} \tag{31}$$

and the group velocity

$$c_g = \frac{-(3 - \beta k^2) \alpha_1 k^2 + (5 - 3\beta k^2) \alpha_2 \beta k^4}{(\beta k^2 - 1)^2} \tag{32}$$

are expressed.

In order to identify the dispersion type let us introduce the following quantity:

$$D = c_p - c_g = \frac{\left[\alpha_1 - 2\alpha_2 \beta k^2 + \alpha_2 \beta^2 k^4 \right] 2k^2}{(\beta k^2 - 1)^2}. \tag{33}$$

In case $D > 0$, the dispersion is normal, in case $D < 0$, the dispersion is anomalous and the case $D = 0$ corresponds to a nondispersive case. It is clear that the sign of D depends on material parameters α_1, α_2 and β as well as on the wavenumber k. If in a certain domain of parameters α_1, α_2 and β, function D is non zero for any value of the wavenumber k, then one has pure normal or pure anomalous dispersion case, i.e., the character of dispersion does not depend on the wavenumber

31

k. Otherwise, the character of dispersion depends on the wavenumber k and this can be called a mixed dispersion case.

The sign of D depends on the sign of the quantity

$$R = \alpha_1 - 2\alpha_2\beta k^2 + \alpha_2\beta^2 k^4. \tag{34}$$

According to Eq. (34), the condition $R = 0$ results in a biquadratic equation which can be solved with respect to βk^2:

$$\beta k^2 = 1 \pm \sqrt{1 - \frac{\alpha_1}{\alpha_2}}. \tag{35}$$

It is obvious that βk^2 has real values only if

$$\frac{\alpha_1}{\alpha_2} \leq 1. \tag{36}$$

In other words, for $\alpha_1 \leq \alpha_2$ one has mixed the dispersion case and for $\alpha_1 > \alpha_2$ the pure normal or pure anomalous dispersion case. In case $\beta < 0$, Eq. (35) has two real roots for k if

$$\frac{\alpha_1}{\alpha_2} < 0. \tag{37}$$

In case $\beta > 0$, Eq. (35) has four real roots for k, if $0 \leq \frac{\alpha_1}{\alpha_2} \leq 1$ and two real roots for k if $\frac{\alpha_1}{\alpha_2} < 0$. The dispersion analysis in more details can be found in [43, 44, 45].

It is worth mentioning that the linearised HKdV Eq. (28) differs from the linearised fifth-order KdV-type equation

$$\frac{\partial u}{\partial t} + \alpha \frac{\partial^3 u}{\partial x^3} + \frac{\partial^5 u}{\partial x^5} = 0 \tag{38}$$

by the third-order mixed derivative

$$\beta \frac{\partial^2}{\partial x^2}\left(\frac{\partial u}{\partial t}\right), \tag{39}$$

that plays a significant role in the dispersion relation.

2.6 Solution symmetry

The solutions of the HKdV Eq. (25) have symmetry in the plane of parameters α_1 and α_2 as follows:

$$u(x, t, \alpha_1, \alpha_2) = -u(-x, t, -\alpha_1, -\alpha_2) \tag{40}$$

parameter β is fixed. Based on this, the cases $\alpha_1 > 0$ and $\alpha_2 > 0$ considered here reflect the behaviour of solutions for $\alpha_1 < 0$ and $\alpha_2 < 0$ as well.

2.7 Statement of the problem

This thesis studies wave propagation in dilatant granular materials by the use of the HKdV Eq. (25). The model equation (25) is integrated numerically under a localised initial condition.

The main goals of the present thesis are to:

- simulate numerically propagation and interaction of solitary waves and solitons in granular media, modelled by HKdV Eq. (25), over a wide range of material parameters (dispersion parameters α_1 and α_2 and microstructure parameter β);

- characterise and analyse the space-time behaviour of solutions in the 3-dimensional domain of material parameters;

- define and describe the types of solutions;

- analyse the character of interactions in terms of solitons, i.e., to understand whether solitary waves that emerge from different initial pulses interact elastically or not;

- estimate the influence of the amplitude of the initial solitary wave on the character of the solution;

- find mutual relations between solution types and material parameters α_1, α_2 and β;

- analyse the formation of the wave packets.

Main attention is paid to the formation of solitonic solutions.

3 Numerical method

Several numerical methods have been developed to solve nonlinear evolution equations: finite difference methods, Galerkin method, Hopscotch method, Fourier expansion method, split-step Fourier method, spectral methods, pseudospectral methods (PsM) etc. All the named methods have minor pros and cons that should be considered when used. Different authors have examined the advantages of the pseudospectral method and have compared it to other methods (see [33, 46, 47, 48, 49] and references therein). According to these studies, the pseudospectral method is adequately accurate and stable for solving KdV type equations.

In this thesis the pseudospectral method is used for the numerical integration of the HKdV Eq. (25). In the present Section the essence of the pseudospectral method is described and accuracy measures are introduced.

3.1 Pseudospectral method

In a nutshell, the idea of the PsM is to approximate space derivatives by a certain global method — reducing thereby a partial differential equation to an ordinary differential equation (ODE) — and to apply a certain ODE solver for integration with respect to the time variable. In this thesis space derivatives were found making use of the discrete Fourier transform (DFT),

$$U(k,t) = Fu = \sum_{j=0}^{n-1} u(j\Delta x, t) \exp\left(-\frac{2\pi i j k}{n}\right), \tag{41}$$

where n is the number of space-grid points, $\Delta x = 2\pi/n$ space step, i imaginary unit, $k = 0, \pm 1, \pm 2, \ldots, \pm(n/2-1), -n/2$, and F denotes the DFT. The usual PsM algorithm (derived for $u_t = \Phi(u, u_x, u_{2x}, \ldots, u_{nx})$ type equations) needs to be modified due to the existence of the mixed partial derivative in the HKdV Eq. (25).

First, the HKdV equation is rewritten in the form

$$\left(u + \beta u_{2x}\right)_t + \left(u + 3\beta u_{2x}\right) u_x + \left(\alpha_1 + \beta u\right) u_{3x} + \beta \alpha_2 u_{5x} = 0 \tag{42}$$

and a variable

$$v = u + \beta u_{2x} \tag{43}$$

is introduced. Making use of the Fourier transform, the last expression can be rewritten in the form

$$v = F^{-1}\left[F(u)\right] + \beta F^{-1}\left[-k^2 F(u)\right] = F^{-1}\left[\left(1 - \beta k^2\right) F(u)\right] \tag{44}$$

where F^{-1} denotes the inverse Fourier transform. From Eq. (44), the variable u can be expressed in the form

$$u = F^{-1}\left[\frac{F(v)}{1 - \beta k^2}\right]. \tag{45}$$

Now the space derivatives of u can be expressed in terms of v

$$\frac{\partial^n u}{\partial x^n} = F^{-1}\left[\frac{(ik)^n F(v)}{1-\beta k^2}\right]. \tag{46}$$

Substituting Eq. (43) into Eq. (42) and expressing the time derivative v_t the following equation results:

$$v_t = -(u+3\beta u_{2x})u_x - (\alpha_1 + \beta u)u_{3x} - \alpha_2\beta u_{5x}. \tag{47}$$

In Eq. (47) the variable u and all its space derivatives could be expressed in terms of v according to expressions (45) and (46). Therefore, Eq. (47) can be considered as an ODE with respect to the variable v and could be integrated numerically by the use of the standard ODE solvers.

Calculations were carried out using SciPy package [50]: for DFT the FFTW [51] library and for ODE solver the F2PY [52] generated Python interface to ODEPACK Fortran code [53] was used. Numerical results were analysed and the figures were generated with Matlab.

3.2 Accuracy and stability of the numerical scheme

The question about the stability and accuracy of solutions certainly arises with any numerical computation. The studied HKdV Eq. (25) can be rewritten in the form of the first conservation law

$$(u+\beta u_{2x})_t + \left[\frac{u^2}{2} + \alpha_1 u_{2x} + \beta\left(\frac{u^2}{2} + \alpha_2 u_{2x}\right)_{2x}\right]_x = 0 \tag{48}$$

with conserved density

$$C_1(t) = \int_0^{2\pi} (u+\beta u_{2x})\,dx \tag{49}$$

and in the form of the second conservation law

$$\left\{\frac{1}{2}\alpha_1 u^2 + \beta\left[(u_x)^2 + u\,u_{2x}\right]\right\}_t + \left\{\frac{1}{3}\alpha_1 u^3 + u\,u_{2x} - \frac{1}{2}(u_x)^2 + \beta\left[\frac{1}{3}\alpha_1 u^3 + u\,u_{2x} - \frac{1}{2}(u_x)^2\right]_{2x}\right\}_x = 0 \tag{50}$$

with conserved density

$$C_2(t) = \int_0^{2\pi} \left\{\frac{1}{2}\alpha_1 u^2 + \beta\left[(u_x)^2 + u\,u_{2x}\right]\right\}dx. \tag{51}$$

35

The values of conserved densities C_1 and C_2 are used for validating the accuracy of the numerical integration. In addition to that, the number of space grid points is a critical measure for the accuracy of the solution. In order to ensure the accuracy of the numerical results, simulations were carried out for a different number of space grid points for fixed values of parameters α_1, α_2, β and A. The calculated wave profiles, were compared in order to determine the lowest value of space grid points where the wave profiles coincided with the results of the higher values of space grid points and the conserved densities C_1 and C_2 were sufficiently accurate.

4 Emergence of solitons and solitary waves

In this Section we simulate the emergence of solitons and solitary waves in dilatant granular materials making use of HKdV Eq. (25). Numerical integration is based on the pseudospectral method, see section 3.1. Simulations are based on the single sech^2–type initial excitation and periodic boundary conditions. Based on the numerical results five different solution types are detected:

1. Single KdV soliton;

2. KdV soliton ensemble;

3. KdV soliton ensemble with a weak tail;

4. Soliton with strong a tail;

5. Solitary wave with a tail and a wave packet.

4.1 Initial and boundary conditions

In order to simulate numerically the propagation of solitary waves in dilatant granular materials the HKdV Eq. (25) is integrated numerically under sech^2-type localised initial conditions

$$u(x,0) = A \operatorname{sech}^2 \frac{x}{\delta}, \quad \delta = \sqrt{\frac{12\alpha_1}{A}}, \tag{52}$$

and periodic boundary conditions

$$u(x + 16k\pi, t) = u(x, t), \quad k = \pm 1, \pm 2, \pm 3, \ldots \tag{53}$$

where A is the amplitude and δ the width of the initial pulse. It is clear that the latter is the analytical solution of the KdV equation that corresponds to the first KdV operator in Eq. (25) [2].

4.2 Accuracy and stability of numerical integration

In order to estimate the accuracy of computations, numerical experiments were carried out with a number of space-grid points $n = 512$, 1024, 2048, 4096. The behaviour of the first and the second conserved density, (49) and (51), respectively, was traced and final wave-profiles $u\left(x, t_f\right)$, i.e., the wave-profiles at the end of the integration interval $t = t_f$, were compared. It was found that final wave-profiles for $n \geq 1024$ practically coincide and therefore in the numerical experiments below the number of space-grid points $n = 1024$ is used.

In all the cases discussed below, the relative error of the conserved density $C_1(t)$ is less than 10^{-7}. The relative error for $C_2(t)$ is less than 10^{-7} in most cases, however, for some sets of parameters, when relatively sharp wave-profiles emerge, relative error for C_2 can have values of order 10^{-2}.

4.3 Solution types

The HKdV Eq. (25) is integrated numerically under initial and boundary conditions (52) and (53), for $0 < \alpha_1 < 1$, $0 < \alpha_2 < 1$ and $\beta = 111.11$, 11.111, 1.111, 0.111, 0.0111. The number of space grid points $n = 1024$ and the length of the time interval $t_f = 100$. In Subsections 4.3.1–4.3.5 all solution types are introduced and described. Results of the numerical studies described in this Section are published in **Publications I**, **II**, and **III**. Additional examples of numerical results can be found in **Report I**.

4.3.1 The first solution type: single KdV soliton

The first solution type is a single KdV soliton, i.e., a single KdV soliton emerges over time. This solution appears in all cases where both dispersion parameters α_1 and α_2 have equal values. The different values of the initial amplitude A or the microstructure parameter β do not change this behaviour. As Eq. (25) consists of two KdV operators that are tight through the second derivative and as the initial condition is the analytical solution of the KdV equation, the solution is quite well predictable. In Figs. 9–11 an example of equal parameters α_1 and α_2 is presented. The KdV soliton propagates with constant amplitude, see Fig. 11, and constant
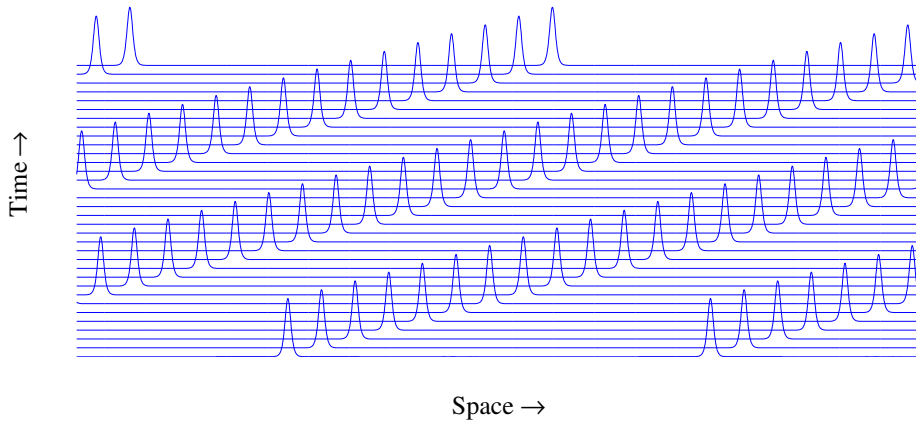
Figure 9: Single KdV soliton. Time–slice plot over two space periods for $\alpha_1 = 0.07$, $\alpha_2 = 0.07$, $\beta = 11.111$, $A = 4$

speed, see corresponding time-slice plot in Fig. 9 and the pseudocolour plot in Fig. 10. The solution could be defined to be a soliton as the initial condition is the analytical solution of the KdV equation.

4.3.2 The second solution type: KdV soliton ensemble

In the case of the second solution type, a train of KdV solitons emerges. The number of generated solitons depends on the values of the macrostructure dispersion parameter α_1 and the microstructure dispersion parameter α_2.

38

Figure 10: Single KdV soliton. Pseudo-colour plot over two space periods for $\alpha_1 = 0.07$, $\alpha_2 = 0.07$, $\beta = 11.111$, $A = 4$
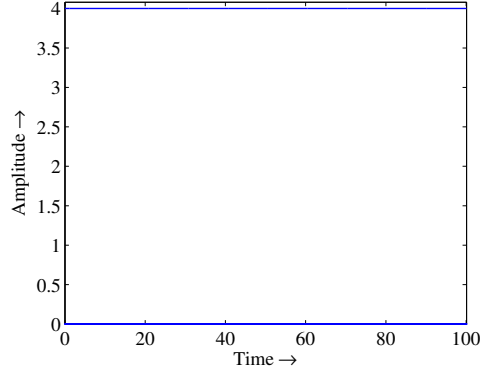
Figure 11: Single KdV soliton. Soliton amplitude against time in case $\alpha_1 = 0.07$, $\alpha_2 = 0.07$, $\beta = 11.111$, $A = 4$

In the given example, see Figs. 12–13, the dispersion parameters have values $\alpha_1 = 0.4$ and $\alpha_2 = 0.01$, resulting in the nine interacting solitons in the ensemble. In the present case the amplitudes of the higher (when one has two solitons in
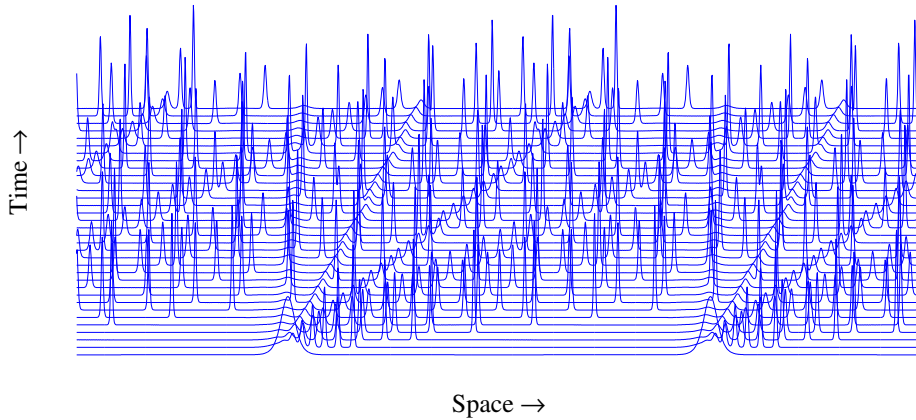
Figure 12: KdV soliton ensemble. Time–slice plot over two space periods for $\alpha_1 = 0.4$, $\alpha_2 = 0.01$, $\beta = 111.11$, $A = 4$

the train) or the highest (when the number of solitons in the train is higher than two) KdV soliton always increase compared to the initial amplitude A, see Fig. 14. Such a behaviour is typical for the KdV equation — if a train of solitons (and a tail) emerges from the initial localised pulse, then the amplitude of the highest soliton in the train is always higher than the amplitude of the initial pulse [11].

Based on the analysis, the number of solitons in the soliton ensemble decreases up to a limit value 1 if α_1 is fixed and α_2 increases or if α_2 is fixed and α_1 decreases (see Subsection 4.4). In the opposite case the number of solitons in the KdV ensemble increases.

39
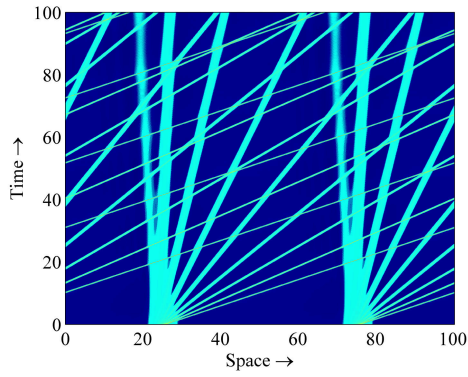
Figure 13: KdV soliton ensemble. Pseudocolour plot over two space periods for $\alpha_1 = 0.4$, $\alpha_2 = 0.01$, $\beta = 111.11$, $A = 4$
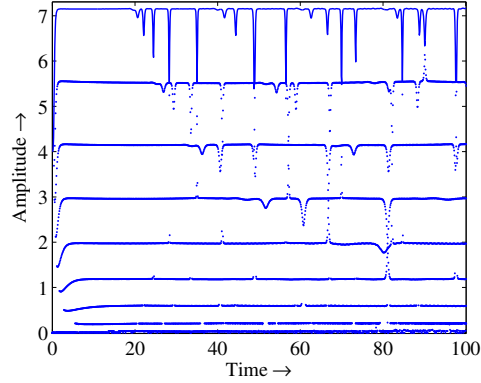
Figure 14: KdV soliton ensemble. Wave-profile maxima against time in case $\alpha_1 = 0.4$, $\alpha_2 = 0.01$, $\beta = 111.11$, $A = 4$

The elastic interactions of KdV solitons are clearly visible, see amplitude curves in Fig. 14 and the corresponding time-slice plot in Fig. 12 and the pseudocolour plot in Fig 13. The solution type is a soliton ensemble as the interactions are elastic, i.e., KdV solitons restore their shape and speed after interactions.

4.3.3 The third solution type: KdV soliton ensemble with a weak tail

In the case of the third solution type a train of KdV solitons and a weak tail emerge. The number of KdV solitons in the ensemble depends on dispersion parameters α_1 and α_2 by the same rule as in the case of the second solution type — if α_2 is fixed and α_1 increases, then the number of solitons in the KdV ensemble increases and vice versa. The weakness of the tail is expressed through the fact that the tail does not influence the behaviour of the KdV ensemble essentially, i.e., here the behaviour of the KdV ensemble is similar to that of the second solution type. In Figs. 15–18 an example of this solution type is presented. In the present case the amplitude of the highest KdV soliton increases compared with the initial amplitude which is typical of the KdV equation behaviour, similarly described in subsection 4.3.2. The interactions of KdV solitons are visible but additionally the maxima that correspond to the tail are visible near the zero level of the amplitude, see Fig. 18 and the corresponding time-slice plot in Fig. 15. The tail causes small variations in the amplitude curves, but does not change the main character of the KdV soliton ensemble – the interactions between the KdV solitons remain (almost) elastic. Formation of the solution and elastic interactions between solitons can be traced in Figs. 15, 16 and 17, where the shape and the size of the tail are clearly visible. The solution type is a soliton ensemble as the solitons in the train interact with each other and restore their shape and speed after the interactions.

40
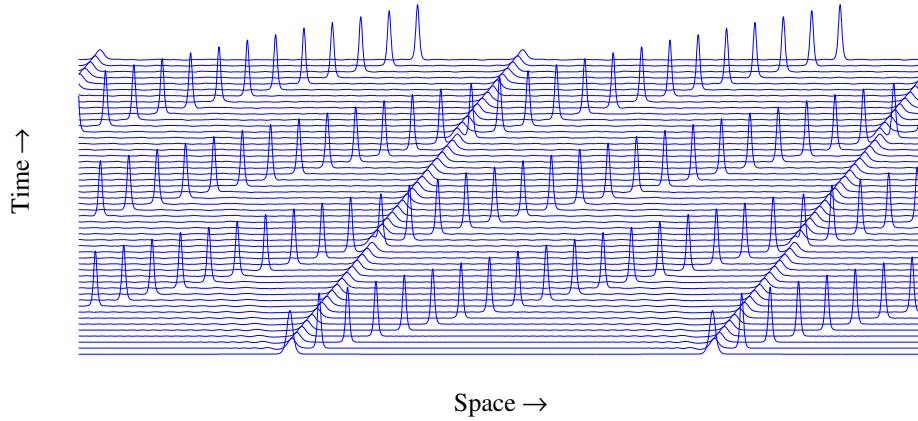
Figure 15: KdV soliton ensemble with a weak tail. Time–slice plot over two space periods for $\alpha_1 = 0.07$, $\alpha_2 = 0.03$, $\beta = 11.111$, $A = 4$
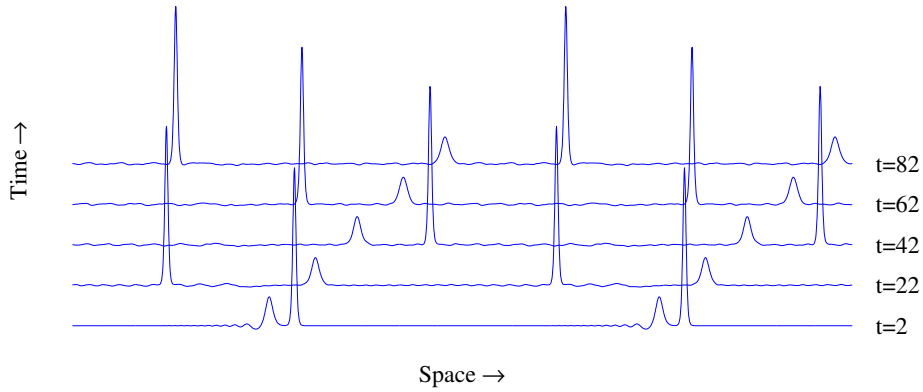
Figure 16: KdV soliton ensemble with a weak tail. Single wave-profiles at $t = 2$, $t = 22$, $t = 42$, $t = 62$, $t = 82$ over two space periods for $\alpha_1 = 0.07$, $\alpha_2 = 0.03$, $\beta = 11.111$, $A = 4$

4.3.4 The fourth solution type: soliton with a strong tail

In the case of the fourth solution type a single soliton and a strong tail emerge. The number of generated oscillations in the tail depends on the values of the macro-structure dispersion parameter α_1 and the microstructure dispersion parameter α_2.

In Figs. 19–22 an example of this solution type is presented. In Figs. 19, 21 and 22 the formation of the solution and interaction between the soliton and the tail can be identified. The size and the shape of the tail can be estimated in Fig. 20. There is always only one solitary wave, which propagates with a decreased ampli-tude compared to the initial amplitude and it oscillates about a certain constant level, see Fig. 22 and the corresponding time-slice plot in Fig. 19. The behaviour of the solution is strongly influenced by the tail: (i) amplitude of the propagating
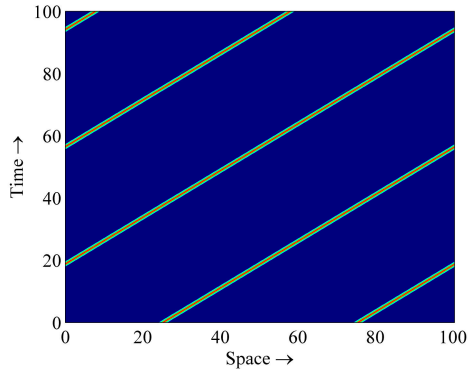
41
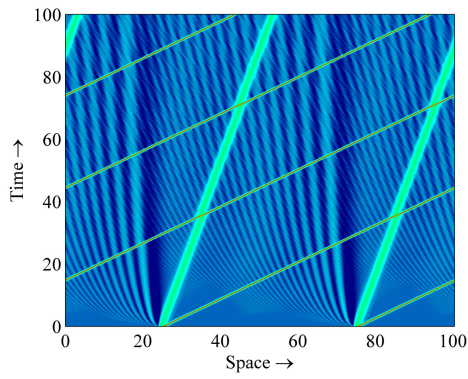
Figure 17: KdV soliton ensemble with a weak tail. Pseudocolour plot over two space periods for $\alpha_1 = 0.07$, $\alpha_2 = 0.03$, $\beta = 11.111$, $A = 4$
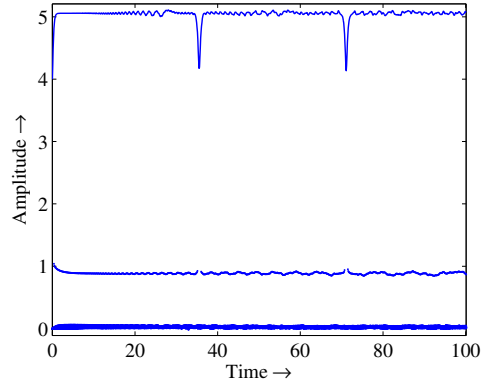
Figure 18: KdV soliton ensemble with a weak tail. Wave-profile maxima against time in case $\alpha_1 = 0.07$, $\alpha_2 = 0.03$, $\beta = 11.111$, $A = 4$
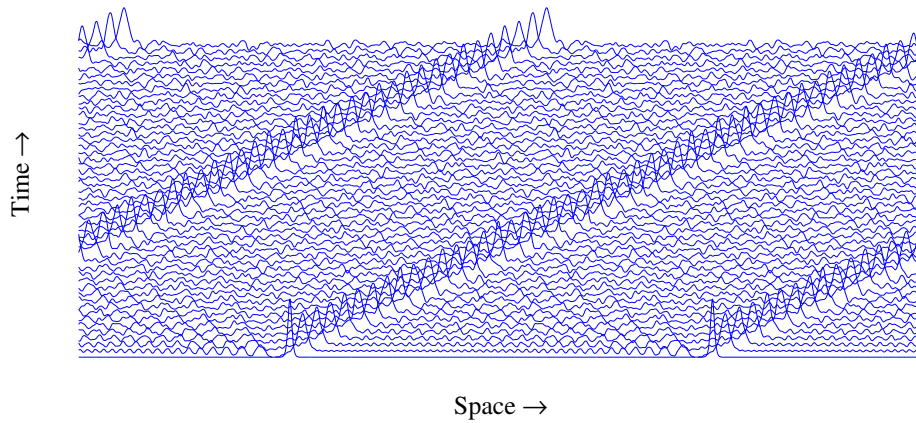
Figure 19: Soliton with a strong tail. Time–slice plot over two space periods for $\alpha_1 = 0.03$, $\alpha_2 = 0.09$, $\beta = 11.111$, $A = 4$

solitary wave is lower than the initial amplitude; (ii) amplitude of the propagating solitary wave is not constant, but due to the influence of the tail it oscillates about a constant level (see Fig. 22). Such a phenomenon — the shape of the initial wave is modified in a way to be more appropriate to the actual solution of the equation — is called selection. In other words, selection means that during propagation the amplitude and the velocity of the initial solitary wave tend to the finite values prescribed by the equation coefficients (see [24, 54, 55, 56] for details). Based on the fact that there is only one propagating solitary wave with a tail, the interactions of the solitary waves do not appear, i.e., we cannot identify the solitonic essence of the fourth solution type and have to do additional analysis, as described in Section 5.

42
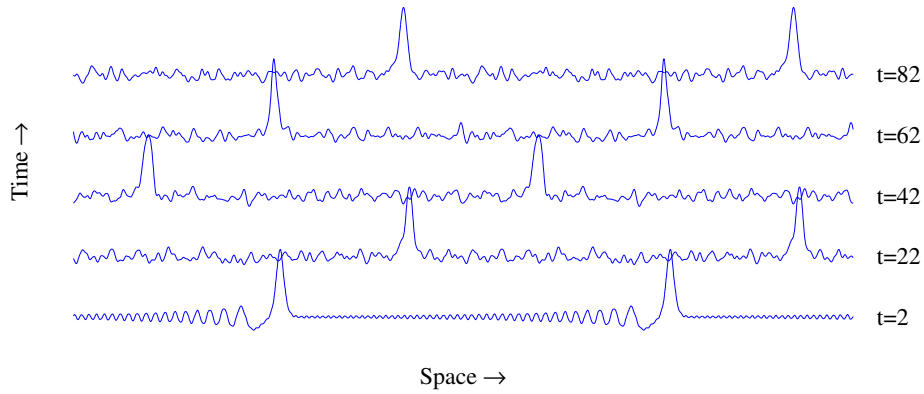
Figure 20: Soliton with a strong tail. Single wave-profiles at $t = 2$, $t = 22$, $t = 42$, $t = 62$, $t = 82$ over two space periods for $\alpha_1 = 0.03$, $\alpha_2 = 0.09$, $\beta = 11.111$, $A = 4$
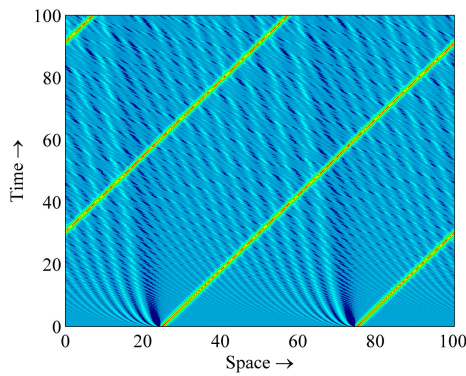
Figure 21: Soliton with a strong tail. Pseudocolour plot over two space periods for $\alpha_1 = 0.03$, $\alpha_2 = 0.09$, $\beta = 11.111$, $A = 4$
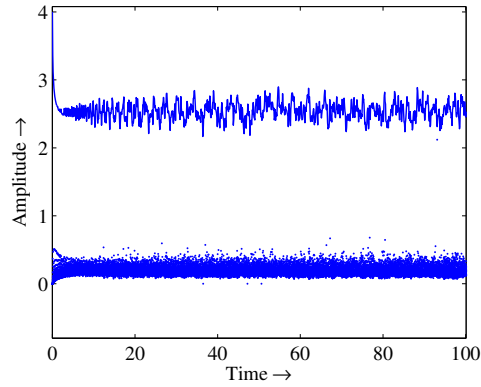
Figure 22: Soliton with a strong tail. Wave-profile maxima against time in case $\alpha_1 = 0.03$, $\alpha_2 = 0.09$, $\beta = 11.111$, $A = 4$

4.3.5   The fifth solution type: solitary wave with a tail and a wave packet

In the case of the fifth solution type, one solitary wave, a tail and wave packet(s) emerge simultaneously (see Figs. 23–26). A similar situation is described by Christov and Velarde in [54]. The wave packet is formed by several amplified higher harmonics (see subsection 4.6 for detailed description). The envelope of the packet can propagate to the left or to the right and at much higher speed than that of the solitary wave or high frequency waves that form the packet. The solution is stable, i.e., all three components of the solution are conserved over long time intervals. As a rule, three different interactions take place in the present case: (i) solitary wave — tail; (ii) solitary wave — wave packet; (iii) tail — wave packet. Furthermore, in some cases two or more wave packets that propagate at different speeds emerge and therefore interactions between wave packets can take place. Like in the case of the fourth solution type, the selection phenomenon [24, 54, 55, 56] takes place.

43
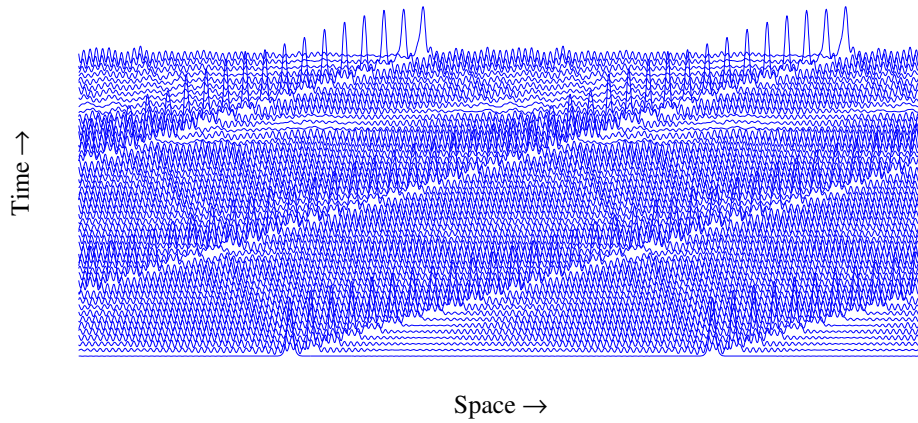
Figure 23: Solitary wave with a tail and a wave packet. Time–slice plot over two space periods for $\alpha_1 = 0.05$, $\alpha_2 = 0.07$, $\beta = 0.0111$, $A = 4$
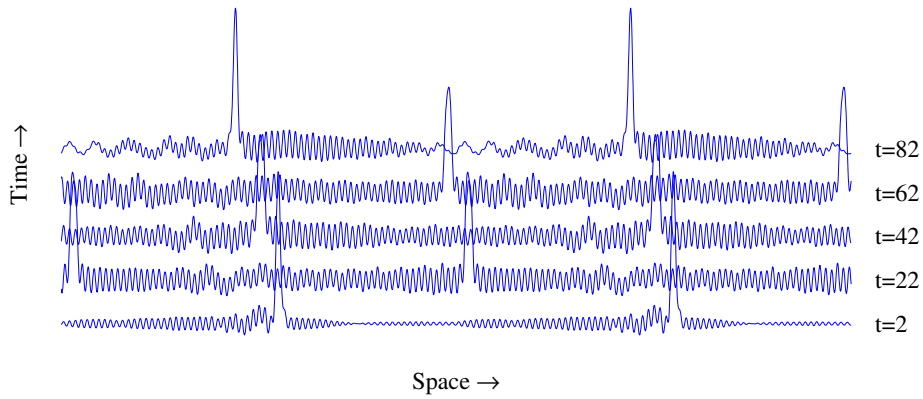
Figure 24: Solitary wave with a tail and a wave packet. Single wave-profiles at $t = 2$, $t = 22$, $t = 42$, $t = 62$, $t = 82$ over two space periods for $\alpha_1 = 0.05$, $\alpha_2 = 0.07$, $\beta = 0.0111$, $A = 4$

In the present case, the amplitude of the solitary wave oscillates strongly around a certain constant level, that is lower than the amplitude of the initial pulse, see Fig. 26 and the corresponding timeslice plot in Fig. 23. However, the single solitary wave interacts with the tail and wave packets and (almost) conserves its speed and shape throughout such interactions. In this sense one can say that the behaviour of these solitary waves is 'soliton-like', but in a strict sense one cannot say that their behaviour is solitonic.

44
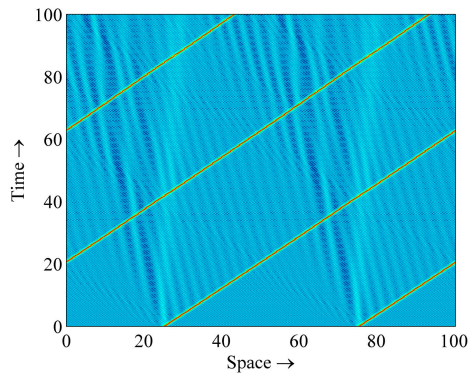
Figure 25: Solitary wave with a tail and a wave packet. Pseudocolour plot over two space periods for $\alpha_1 = 0.05$, $\alpha_2 = 0.07$, $\beta = 0.0111$, $A = 4$
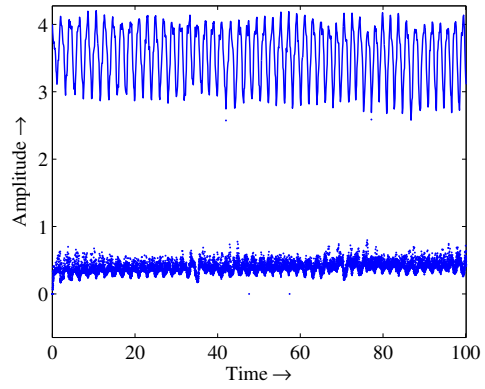
Figure 26: Solitary wave with a tail and a wave packet. Wave-profile maxima against time in case $\alpha_1 = 0.05$, $\alpha_2 = 0.07$, $\beta = 0.0111$, $A = 4$

4.3.6 Limit cases

During the analysis of the numerical results some limit cases where observed: (i) Fig. 27 demonstrates the case where the number of KdV solitons is very high and probably the second KdV ensemble forms; (ii) Fig. 28 demonstrates the case where the solitary wave disappears in wave-profiles, i.e., the amplitude of the solitary wave can be lower than the amplitude of the wave packets.
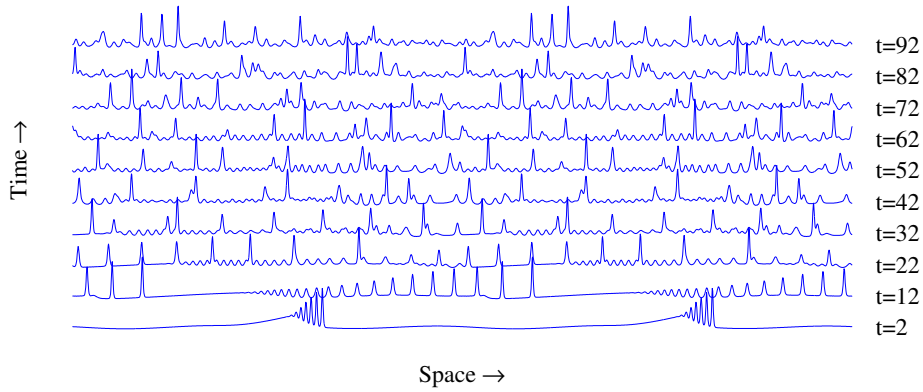
Figure 27: KdV soliton ensemble. Single wave-profiles at $t = 1$, $t = 5$, $t = 10$, $t = 15$, $t = 20$, $t = 30$, $t = 40$, $t = 50$, $t = 60$, $t = 70$ over two space periods for $\alpha_1 = 2.2$, $\alpha_2 = 0.01$, $\beta = 11.111$, $t_f = 500$, $A = 4$
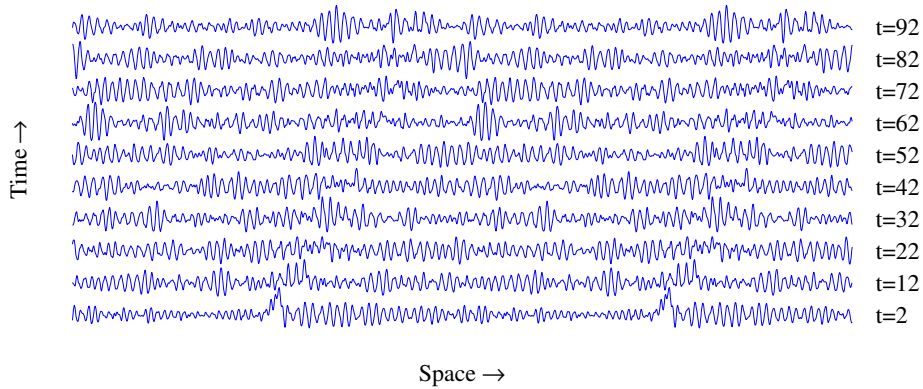
Figure 28: Solitary wave with a tail and a wave packet. Single wave-profiles at $t = 1$, $t = 5$, $t = 10$, $t = 15$, $t = 20$, $t = 30$, $t = 40$, $t = 50$, $t = 60$, $t = 70$ over two space periods for $\alpha_1 = 0.01$, $\alpha_2 = 0.05$, $\beta = 0.0111$, $A = 4$

4.4 Number of solitons and solitary waves

In Figs. 29–33 a number of solitons are presented against the dispersion parameters α_1 and α_2 for different values of the microstructure parameter β. In case $\alpha_1 \le \alpha_2$ there is always only one soliton or solitary wave (except the limit cases when the solitary wave disappears). In case $\beta \ge 1.111$ and $\alpha_1 > \alpha_2$ the number of solitons in the KdV ensemble increases step by step if α_1 increases and α_2 is fixed or if α_2 decreases and α_1 is fixed, see Figs. 29–31. For $\beta \le 0.1111$ the number of solitons is one for $\alpha_1 > \alpha_2$, see Figs. 32 and 33.
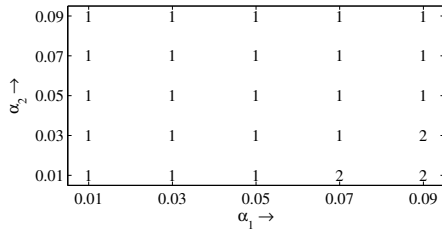
Figure 29: Number of solitons or solitary waves in case $\beta = 111.11$, $A = 4$
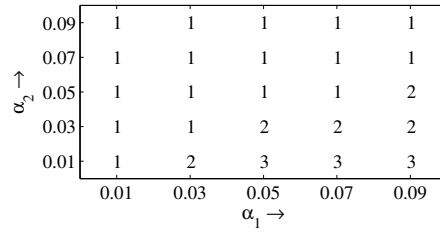
Figure 30: Number of solitons or solitary waves in case $\beta = 11.111$, $A = 4$
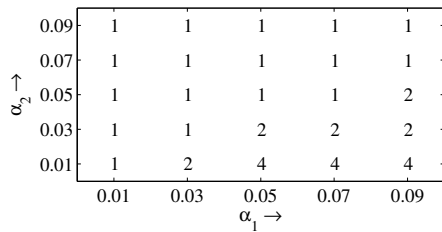
Figure 31: Number of solitons or solitary waves in case $\beta = 1.111$, $A = 4$
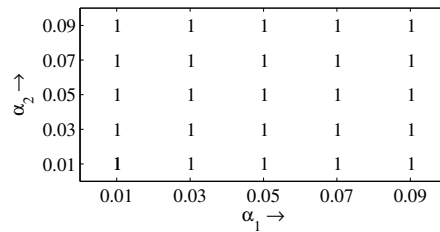
Figure 32: Number of solitons or solitary waves in case $\beta = 0.1111$, $A = 4$
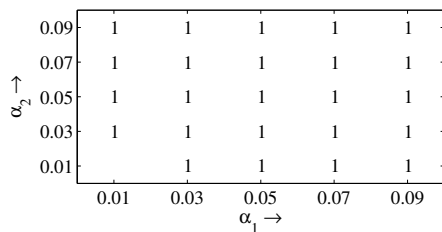
Figure 33: Number of solitons or solitary waves in case $\beta = 0.0111$, $A = 4$

4.5 Influence of the initial amplitude

In this section the influence of the initial amplitude on the solution behaviour is described and analysed. In Figs. 34–51 different solutions with different values of parameters α_1, α_2, β and A are presented.

In the case of the first solution type the increase of the initial amplitude causes the increase in the propagation speed of the KdV soliton. The essence of the solution remains the same, see the corresponding pseudocolour plots in Fig. 34 and 35 for the cases $A = 5$ and $A = 10$.

In the case of the second solution type the increase of the initial amplitude causes the increase of the propagation speed of solitons in the KdV soliton ensemble but the number of solitons in the considered cases did not change, see the corresponding pseudocolour plots in Figs. 36 and 38 with the corresponding amplitude curves in Figs. 37 and 39.

In the case of the third solution type the increase of the initial amplitude causes the increase of propagation speed of KdV solitons. The essence of the solution remains the same for the considered values of amplitude $A = 1$, $A = 5$, $A = 10$ and $A = 15$, see examples in Figs. 40 and 42. The amplitude of the weak tail increases if the initial amplitude increases but it does not alter the solution type, see examples in Figs. 41 and 43.

In the case of the fourth solution type the increase of the initial amplitude from $A = 1$ to $A = 15$ causes the increase of the propagation speed of the soliton. The essence of the solitary wave and the tail does not change, see the example of pseudocolour plots in Figs. 44 and 46, the corresponding wave–profile amplitude curves are in Figs. 45 and 47.

In the case of the fifth solution type the increase of the initial amplitude causes more complex changes than in previous cases — propagation speed of the solitary wave and the shape of its trajectory is altered, see examples for $A = 5$ in Figs. 48 and 49 and for $A = 10$ in Figs. 50 and 51. However, the solution type does not change.

More examples of the solutions on different amplitude levels but on the constant set of parameters α_1, α_2 and β can be found in **Report I**. Table 1 summarises the increase of the propagation speed of the highest soliton or solitary wave in the case of an increased value of the initial amplitude. In all cases the speed of the (highest) solitary wave increases if the initial amplitude increases.
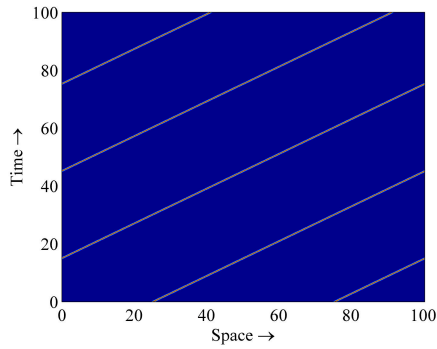
Figure 34: Single KdV soliton. Pseudo-colour plot over two space periods for $\alpha_1 = 0.05$, $\alpha_2 = 0.05$, $\beta = 1.111$, $A = 5$
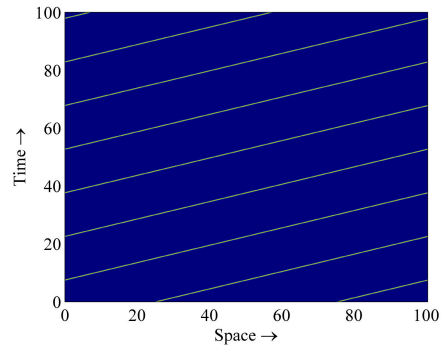
Figure 35: Single KdV soliton. Pseudo-colour plot over two space periods for $\alpha_1 = 0.05$, $\alpha_2 = 0.05$, $\beta = 1.111$, $A = 10$
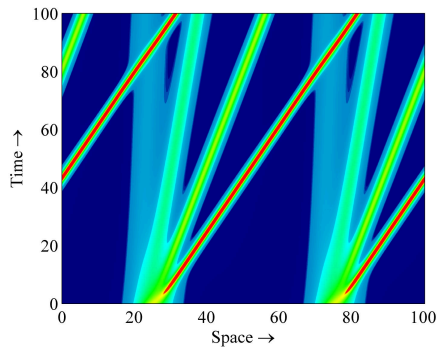
Figure 36: KdV soliton ensemble. Pseudocolour plot over two space periods for $\alpha_1 = 1$, $\alpha_2 = 0.1$, $\beta = 111.11$, $A = 1$
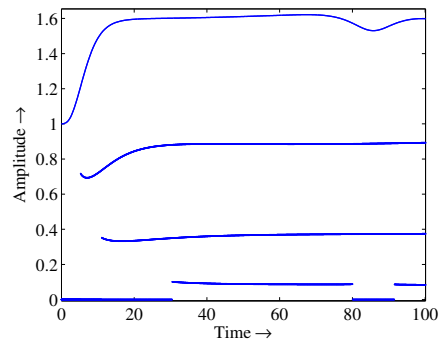
Figure 37: KdV soliton ensemble. Wave-profile maxima against time in case $\alpha_1 = 1$, $\alpha_2 = 0.1$, $\beta = 111.11$, $A = 1$
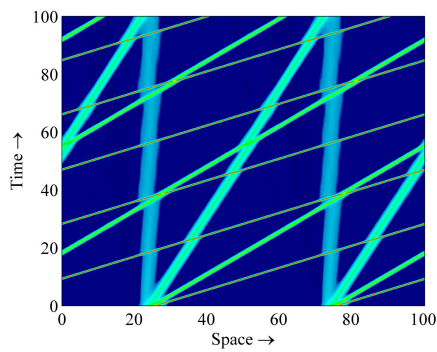
Figure 38: KdV soliton ensemble. Pseudocolour plot over two space periods for $\alpha_1 = 1$, $\alpha_2 = 0.1$, $\beta = 111.11$, $A = 5$
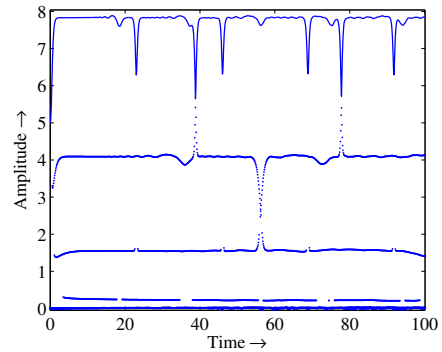
Figure 39: KdV soliton ensemble. Wave-profile maxima against time in case $\alpha_1 = 1$, $\alpha_2 = 0.1$, $\beta = 111.11$, $A = 5$

49
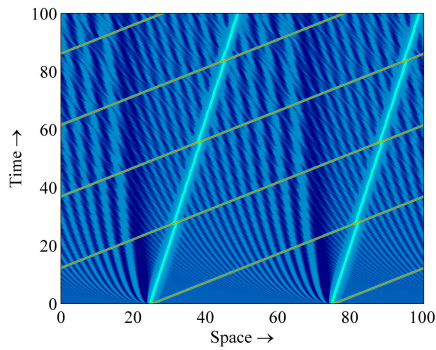
Figure 40: KdV soliton ensemble with a weak tail. Pseudocolour plot over two space periods for $\alpha_1 = 0.1$, $\alpha_2 = 0.05$, $\beta = 111.11$, $A = 5$
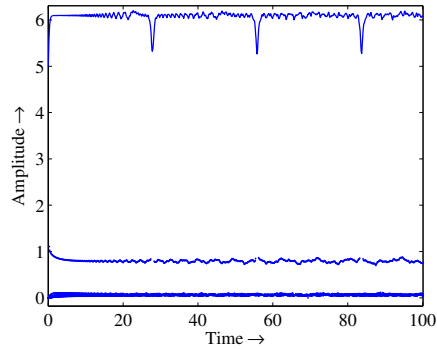
Figure 41: KdV soliton ensemble with a weak tail. Wave-profile maxima against time in case $\alpha_1 = 0.1$, $\alpha_2 = 0.05$, $\beta = 111.11$, $A = 5$
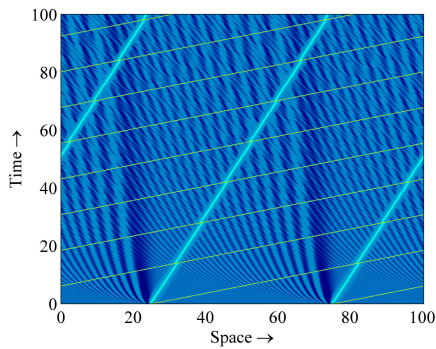
Figure 42: KdV soliton ensemble with a weak tail. Pseudocolour plot over two space periods for $\alpha_1 = 0.1$, $\alpha_2 = 0.05$, $\beta = 111.11$, $A = 10$
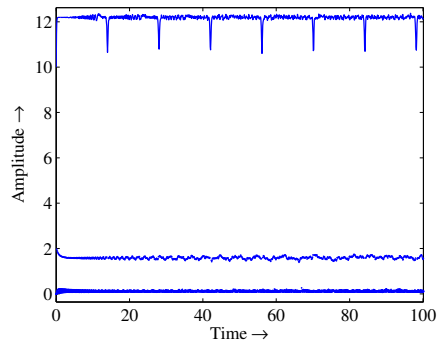
Figure 43: KdV soliton ensemble with a weak tail. Wave-profile maxima against time in case $\alpha_1 = 0.1$, $\alpha_2 = 0.05$, $\beta = 111.11$, $A = 10$
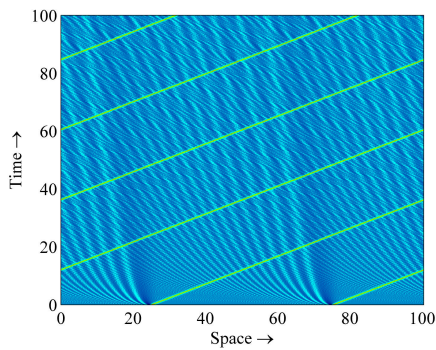
Figure 44: Soliton with a strong tail. Pseudocolour plot over two space periods for $\alpha_1 = 0.03$, $\alpha_2 = 0.09$, $\beta = 11.111$, $A = 10$
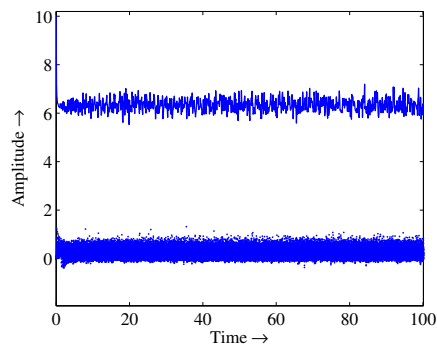
Figure 45: Soliton with a strong tail. Wave-profile maxima against time in case $\alpha_1 = 0.03$, $\alpha_2 = 0.09$, $\beta = 11.111$, $A = 10$
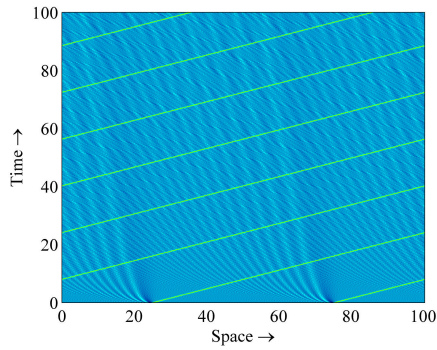
Figure 46: Soliton with a strong tail. Pseudocolour plot over two space periods for $\alpha_1 = 0.03$, $\alpha_2 = 0.09$, $\beta = 11.111$, $A = 15$
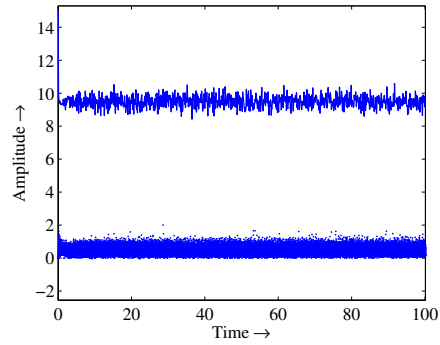
Figure 47: KdV soliton with a strong tail. Wave-profile maxima against time in case $\alpha_1 = 0.03$, $\alpha_2 = 0.09$, $\beta = 11.111$, $A = 15$
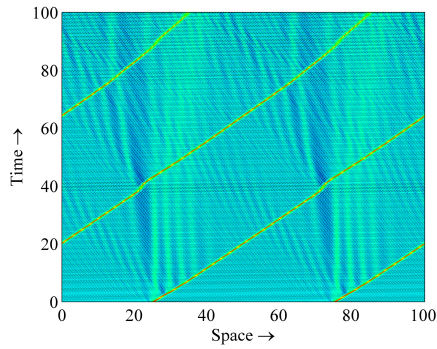
Figure 48: Solitary wave with a tail and a wave packet. Pseudocolour plot over two space periods for $\alpha_1 = 0.05$, $\alpha_2 = 0.07$, $\beta = 0.0111$, $A = 5$
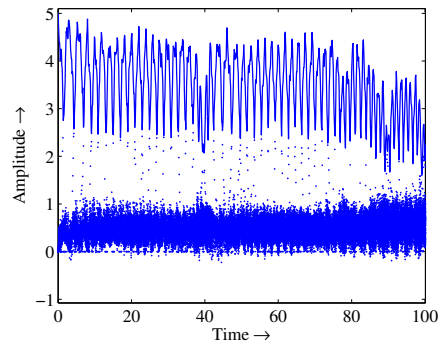
Figure 49: Solitary wave with a tail and a wave packet. Wave-profile maxima against time in case $\alpha_1 = 0.05$, $\alpha_2 = 0.07$, $\beta = 0.0111$, $A = 5$
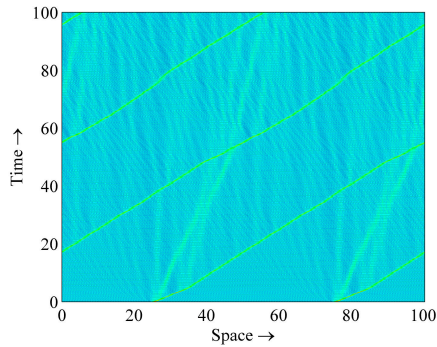
Figure 50: Solitary wave with a tail and a wave packet. Pseudocolour plot over two space periods for $\alpha_1 = 0.05$, $\alpha_2 = 0.07$, $\beta = 0.0111$, $A = 10$
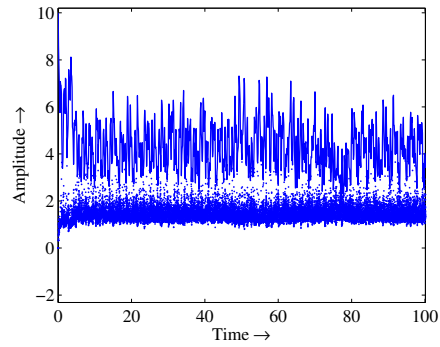
Figure 51: Solitary wave with a tail and a wave packet. Wave-profile maxima against time in case $\alpha_1 = 0.05$, $\alpha_2 = 0.07$, $\beta = 0.0111$, $A = 10$

Table 1: The speed of the highest soliton or solitary wave against the initial amplitude A and solution type

	Parameters			Speed		
Type	α_1	α_2	β	$A=1$	$A=5$	$A=10$
1	0.05	0.05	1.111	0.33	1.65	3.26
2	1	0.1	111.11	0.58	2.65	5.13
3	0.1	0.05	111.11	0.41	2.01	3.99
4	0.03	0.09	11.111	0.23	1.03	2.04
5	0.1	0.05	0.1111	0.31	1.17	2.17

4.6 Wave packet phenomenon and spectral quantities

In this Section the fifth solution type and the wave packet phenomenon are discussed in terms of spectral quantities. For this reason spectral densities and time averaged normalised spectral densities are defined. The idea of applying time averaged normalised spectral densities comes from Galgani et al. [57] where time averaged energies of single modes are used in order to discuss the energy equipartition in systems of the FPU type.

If $U(k,t)$ is the DFT of function $u(x,t)$ defined by expression (41), then spectral densities

$$
S(k,t) = \frac{4\big[U(k,t)\big]^2}{n^2}, \quad k = 1,...,\frac{n}{2} - 1,
$$
$$
S(k,t) = \frac{2\big[U(k,t)\big]^2}{n^2}, \quad k = \frac{n}{2}.
$$
(54)

For each value of t one can define the sum of spectral densities

$$
S_{\mathrm{sum}}(t) = \sum_{k=1}^{n/2} S(k,t),
$$
(55)

normalised spectral densities

$$
S_{\mathrm{norm}}(k,t) = \frac{S(k,t)}{S_{\mathrm{sum}}(t)} \cdot 100\%
$$
(56)

and time averaged normalised spectral densities (TANSD)

$$
S_{\mathrm{a}}(k,t) = \frac{\int_0^t S_{\mathrm{norm}}(k,t)\,dt}{t}.
$$
(57)

We have discrete values of spectral densities S and S_{norm} at discrete time moments t_i, i.e., we have $S(k,t_i)$ and $S_{\mathrm{norm}}(k,t_i)$. Therefore at $t = t_i$

$$
S_{\mathrm{a}}(k,t_i) = \frac{\sum_{m=1}^{i} S_{\mathrm{norm}}(k,t_m)}{i}.
$$
(58)

TANSD (58) reflect the contribution of the k-th spectral density over the time interval $[0,t_i]$. In contrast to spectral densities, TANSD curves provide a clearer comprehension of the domination of certain harmonics.

In the case of the first four solution types, no dominating spectral densities exist. For example, in Fig. 52 time averaged spectral densities are plotted for the third solution type (KdV soliton ensemble with a weak tail, see the corresponding time–slice plot in Fig. 12). One can see that at $t = 100$ all time averaged spectral densities have values below 2. In the case of the fifth solution type — a solitary
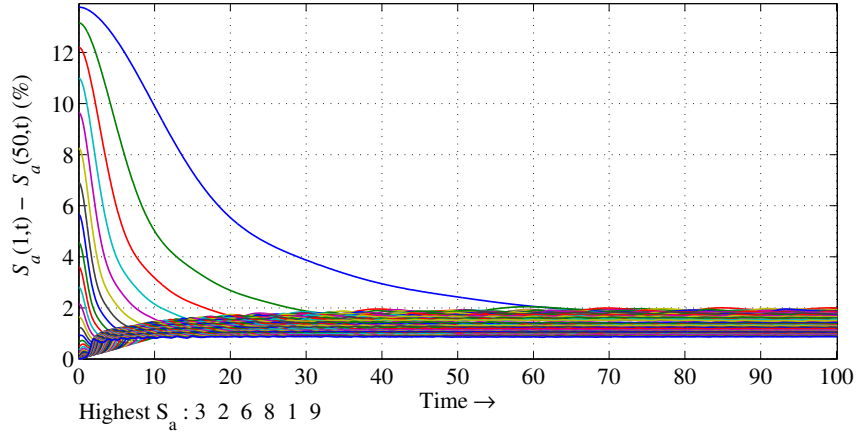
Figure 52: KdV soliton ensemble with a weak tail. Time averaged normalised spectral densities in case $\alpha_1 = 0.4$, $\alpha_2 = 0.01$, $\beta = 111.11$, $A = 4$

wave with a tail and a wave packet — the behaviour of TANSD is completely different. In Fig. 53 the corresponding time-slice plot is presented for $\alpha_1 = 0.05$, $\alpha_2 = 0.09$, $\beta = 0.0111$. TANSD in Fig. 54 demonstrates that $S_a(60, 100) > 40$, $S_a(61, 100) \approx 12.5$, $S_a(59, 100) \approx 11$, $S_a(62, 100) \approx 2.5$ and other TANSD have values less than 2 at $t = 100$, i.e., 59th–62nd spectral densities are amplified and dominate over the others in time interval [0,100]. It is clear that wave packets are formed by
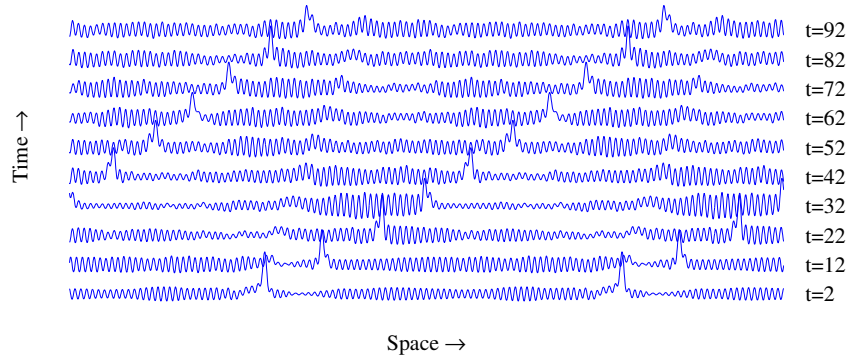
Figure 53: Solitary wave with a tail and a wave packet. Time–slice plot over two space periods for $\alpha_1 = 0.05$, $\alpha_2 = 0.09$, $\beta = 0.0111$, $A = 4$

amplified harmonics and S_a having the highest value determines the number of maxima (oscillations) in a certain wave-profile. Similar situations are described in many textbooks (see [58], for example) in order to explain group velocity and dispersion phenomena — sum of harmonic waves having nearly equal frequencies presents a wave packet.

In the limit case, only one spectral density is dominating and envelope waves (typical of wave packets) are formed only at the beginning of the integration in-
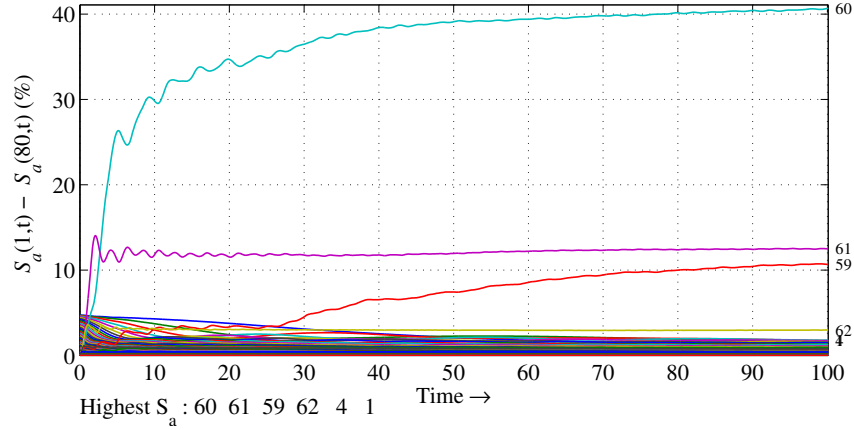
Figure 54: Solitary wave with a tail and a wave packet. Time averaged normalised spectral densities in case $\alpha_1 = 0.05$, $\alpha_2 = 0.09$, $\beta = 0.0111$, $A = 4$

terval. For $t = t_f$ ensemble of (nearly) equal amplitude of (small) solitary waves (EA ensemble for short) [45, 59] is formed between KdV solitons. EA ensemble was found to form in few cases only. For example, in case $\alpha_1 = 0.07$, $\alpha_2 = 0.11$, $\beta = 0.0111$ the 63rd harmonic dominates, see Figs. 55 and 56. The number of the
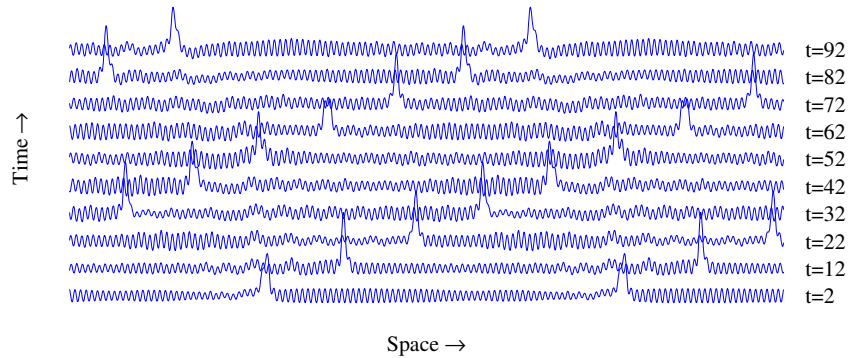
Figure 55: Solitary wave with a tail and a wave packet, limit case: KdV soliton with a tail and EA ensemble. Time–slice plot over two space periods for $\alpha_1 = 0.07$, $\alpha_2 = 0.11$, $\beta = 0.0111$, $A = 4$

dominating harmonic reflects the number of solitary waves in the EA ensemble, i.e., if the 63rd harmonic is dominating, then there are 63 solitary waves in the EA ensemble.

4.7 Discussion

Phenomena described under the fifth solution type could be explained in terms of embedded solitons. Embedded solitons have been identified in a wide array

55
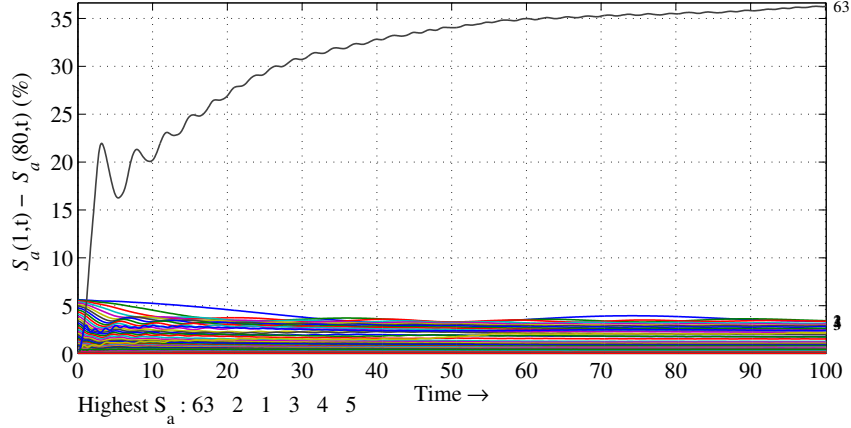
Figure 56: Solitary wave with a tail and a wave packet, limit case: KdV soliton with tail and EA ensemble. Time averaged normalised spectral densities in case $\alpha_1 = 0.07$, $\alpha_2 = 0.11$, $\beta = 0.0111$, $A = 4$

of physical systems, including these described by the generalised fifth-order KdV equations (see [60, 61, 62]). However, in this work periodic boundary conditions are used and therefore related theory for embedded solitons cannot be directly transferred.

To distinguish between the second and the third solution types, i.e., between KdV soliton ensemble and KdV soliton ensemble with a weak tail, is quite conditional. The tail is sometimes so weak that it is practically indistinguishable by means of wave-profile extrema as well as spectral quantities. The situation is likely to be analogous to the KdV equation where the pure N-soliton solution is formed only for a certain fixed values of parameters. In other cases an ensemble of N-solitons and a tail (which can be very small) are formed.

For the KdV equation of form $u_t + u\,u_x + u_{3x} = 0$ initial pulse $u(x,0) = 6N(N+1)\operatorname{sech}^2 x$ results in train on N solitons, where the k-th soliton ($k = 1,\ldots,N$) propagates at the speed $c_k = 4(N+1-k)^2$ and its amplitude $A_k = 3c_k$ [63]. If the amplitude of the initial pulse is denoted by $A_0 = 6N(N+1)$, then ratios $A_k/A_0 = [2(N+1-k)^2]/[N(N+1)]$.

Table 2 presents the ratios of A_k/A_0 for $N = 1\ldots 9$ solitons solutions In Section 4.3.2 an example is discussed, where a train of nine solitons is formed from the initial pulse (52). If soliton amplitudes A_k^{num} are measured near $t = 15$ (i.e. when they are well separated) we obtain $A_k^{\mathrm{num}}/A_0 \approx [1.797, 1.397, 1.048, 0.749, 0.503, 0.305, 0.155, 0.053, 0.011]$ (here $A_0 = 4$). It is clear that these values are very close to values A_k/A_0 for $N = 9$ and therefore the numerical solution considered can be called a KdV soliton ensemble. In Section 4.3.3 we examined a case where two solitons and a weak tail are formed from the initial pulse (52) with $A \equiv A_0 = 4$. Now we obtain $A_k^{\mathrm{num}}/A_0 \approx [1.2614, 0.2424]$. These values are essentially lower than values A_k/A_0 for $N = 2$. However, the situation is again similar to that of the KdV case: if $A_0|_{N=1} < A_0 < A_0|_{N=2}$, then the train of two solitons and a tail is formed, and

56

Table 2: Amplitudes of N solitons for the KdV equation

N	k-th solitons amplitude
	1	2	3	4	5	6	7	8	9
1	1								
2	4/3	1/3							
3	3/2	2/3	1/6						
4	1.6	0.9	0.4	0.1					
5	1.667	1.067	0.6	0.267	0.067				
6	1.714	1.190	0.762	0.429	0.190	0.048			
7	1.750	1.286	0.893	0.571	0.321	0.143	0.036		
8	1.778	1.361	1	0.694	0.444	0.25	0.111	0.028	
9	1.8	1.422	1.089	0.8	0.556	0.356	0.2	0.089	0.022

amplitudes of single solitons $A_k < A_k|_{N=2}$. Finally, remember that the initial condition (52) is one soliton solution of the KdV equation that corresponds to the first KdV operator in Eq. (25) and the formation of soliton trains takes place due to the influence of the second KdV operator in Eq. (25).

In Subsections 4.3.1–4.3.5 solution types were introduced making use of the fixed value $A = 4$ for the amplitude of the initial solitary wave. In Section 4.5 additional numerical experiments for $1 \le A \le 15$ were carried out in order to estimate the influence of the initial amplitude on the character of the solution. It was found that in the case of solution types (i)–(iv) the rise of the initial amplitude increases the speed of emerging solitons but neither the solution type nor the number of solitons in the KdV ensemble changes. In the case of the fifth solution type the increase of the initial amplitude from $A = 1$ to $A = 15$ causes more complex changes than in previous cases. For $A \ge 5$ propagation of the solitary wave is so strongly influenced by the tail and wave packet that its straight-line trajectory is altered to that of a curvilinear one. However, the solution type is not changed (all three solution components of the solution exist over the time interval $0 \le t \le t_f$). The full set of corresponding figures is presented in **Report I**.

According to the analysis above one can conclude that the solitonic character of the solution and the usage of the term 'KdV soliton ensemble' is strictly verified for the second and the third solution types. For these solution types solitary waves conserve their shape and speed throughout interactions with other solitary waves. In other words, the behaviour of these ensembles of solitary waves is practically identical to that of the KdV solitons and therefore the train of solitary waves is termed the 'KdV soliton ensemble'. In the case of the first solution type the initial solitary wave, which is the analytical solution of the KdV equation, propagates at constant speed and amplitude; in the case of the fourth and the fifth solution types, the single solitary wave interacts with the tail and wave packets (in the case of the fifth solution type) and (almost) conserves its speed and shape throughout such interactions. However, in order to discuss the solitonic character more strictly one needs to simulate interactions between these solitary waves. This is elaborated in Section 5.

5 Interactions of solitons and solitary waves

In this Section we simulate the interactions of solitons and solitary waves according to the solution types defined in Section 4:

   (i) KdV solitons;

  (ii) KdV soliton ensembles (with weak tails);

 (iii) Solitons with strong tails;

 (iv) Solitary waves with tails and wave packets.

In order to simulate interactions between solitons, soliton ensembles and solitary waves an appropriate initial condition is used:

   (i) initial condition consists of two sech^2-type localised excitations;

  (ii) sech^2-type localised excitations are shifted with respect to $x = 0$ by 16π and 48π

 (iii) sech^2-type localised excitations have different amplitudes, i.e., they generate solitary waves that propagate at different speeds.

The appropriate initial condition allows us to simulate the interactions of: (i) two single KdV solitons (the first solution type in Section 4); (ii) solitons from different KdV soliton ensembles (the second and the third solution types in Section 4); (iii) two solitons with strong tails (the fourth solution type in Section 4); (iv) two solitary waves with tails and wave packets (the fifth solution type in Section 4) and to analyse the character of interactions in terms of solitons, i.e., to understand whether solitary waves that emerge from different initial pulses interact elastically or not.

The results that are presented in this Section are published in papers **Publications IV** and **V**. Detailed description of the analysis and several additional examples can be found in **Report II**.

5.1 Initial and boundary conditions

In order to simulate interactions between solitons, soliton ensembles and solitary waves an initial condition is used here that consists of two sech^2-type localised waves which are shifted with respect to $x = 0$ by 16π and 48π, respectively:

$$u(x,0) = A_1 \text{sech}^2 \frac{x - 16\pi}{\delta_1} + A_2 \text{sech}^2 \frac{x - 48\pi}{\delta_2} \tag{59}$$

$$\delta_1 = \sqrt{\frac{12\alpha_1}{A_1}}, \quad \delta_2 = \sqrt{\frac{12\alpha_1}{A_2}}.$$

Here A_1 is the amplitude of the left hand side and A_2 is the amplitude of the right hand side sech^2-type pulse, δ_1 and δ_2 are the widths of the initial pulses and $0 \leq x < 64\pi$. Appropriate periodic boundary conditions

$$u(x + 64k\pi, t) = u(x, t), \quad k = \pm 1, \pm 2, \pm 3, \ldots, \tag{60}$$

are applied. The values of dispersion parameters α_1, α_2 and microstructure parameter β have been selected according to the solution types defined in **Publications I**, **II** and **III**. The number of space grid points $n = 4096$ and the length of the time interval $t_f = 100$.

5.2 Accuracy and stability of numerical integration

In order to estimate the accuracy of computations, numerical experiments were carried out with a number of space-grid points $n = 2048, 4096, 8192$. The behaviour of the conserved densities C_1 and C_2 (see Section 3.2) was traced and final wave-profiles $u\left(x, t_f\right)$, i.e., the wave-profiles at the end of the integration interval $t = t_f$, were compared. It was found that final wave-profiles for $n \geq 4096$ practically coincide and therefore in the numerical experiments presented in this Section, the number of space-grid points $n = 4096$ is used. In all the cases discussed below, the relative error of the conserved density $C_1(t)$ is less than 10^{-10} and for $C_2(t)$ less than 10^{-2}.

5.3 Interactions of single KdV solitons

The first solution type is called the single KdV soliton and it appears if dispersion parameters $\alpha_1 = \alpha_2$. In this case the initial sech^2-pulses propagate at constant speed and constant amplitude.

Here we simulate interactions between two initial pulses that have different amplitudes and therefore they propagate at different speeds. The left hand side solitary wave with the amplitude $A_1 = 15$ propagates faster than the right hand side one with the amplitude $A_1 = 5$ and interactions can take place (see the corresponding time-slice, pseudocolour and wave-profile maxima plots in Figs. 57, 58 and 59).

Those figures demonstrate clearly that interactions between solitons are elastic as the solitons restore their speeds and amplitudes after interactions. During the interactions, solitons are phase shifted — the higher amplitude soliton is shifted to the right and the lower amplitude soliton to the left, see pseudocolour plot in Fig. 58.

In order to verify the solitonic character of the solution and the usage of the name 'KdV soliton', the behaviour of the solitons during interactions was compared to the behaviour of solitons in the case of the KdV equation. In the case of two-soliton solution of the KdV equation of the form $u_t + u u_x + d u_{3x} = 0$, the phase-shifts of interacting solitons can be found analytically as follows:

$$\vartheta_1 = \Theta \Delta_1, \quad \vartheta_2 = -\Theta \Delta_2, \quad \Theta = \ln \frac{1 + \sqrt{r}}{1 - \sqrt{r}}, \quad \Delta_i = \sqrt{\frac{12d}{A_i}}, \quad r = \frac{A_2}{A_1}. \tag{61}$$

59

Here ϑ_1, ϑ_2 are phase-shifts of the higher and the lower soliton, respectively and $A_1 > A_2$ are amplitudes of interacting solitons (see [64] for details). In the numerical experiments, velocities and phase-shifts of interacting solitons were calculated making use of trajectories of wave-profile local maxima (in [64] three different types of trajectories are distinguished). One can conclude that (i) between interactions solitons restored their initial amplitudes A_i and speeds $c_i = A_i/3$, and (ii) numerical phase-shifts $\vartheta_i^{\mathrm{num}}$ and phase-shifts (61) coincide. In other words, in case $\alpha_1 = \alpha_2$ initial pulses (59) behave exactly like KdV solitons.
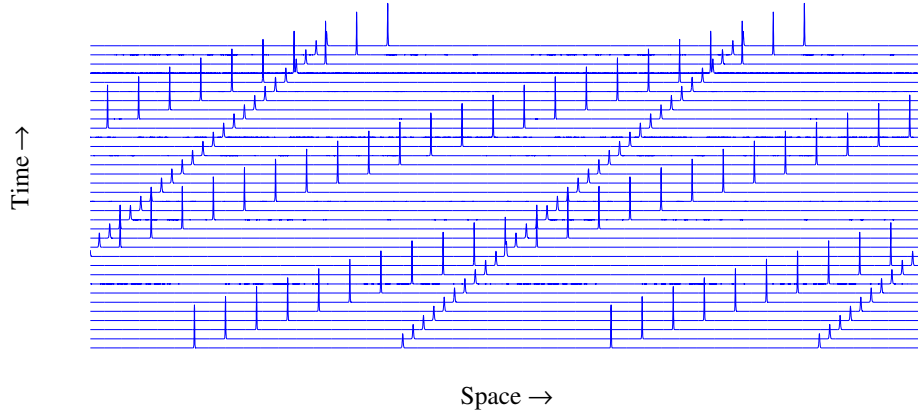
Figure 57: Interactions of KdV solitons. Timeslice plot over two space periods for $\alpha_1 = \alpha_2 = 0.03$, $\beta = 0.0111$, $A_1 = 15$, $A_2 = 5$
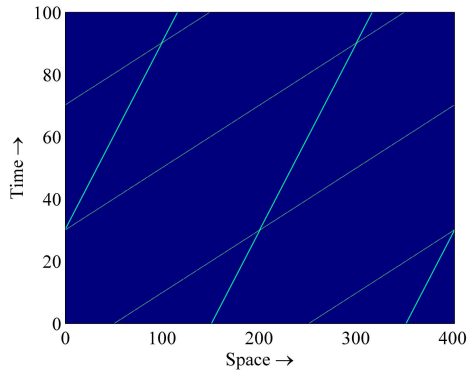
Figure 58: Interactions of KdV solitons. Pseudocolour plot over two space periods for $\alpha_1 = \alpha_2 = 0.03$, $\beta = 0.0111$, $A_1 = 15$, $A_2 = 5$
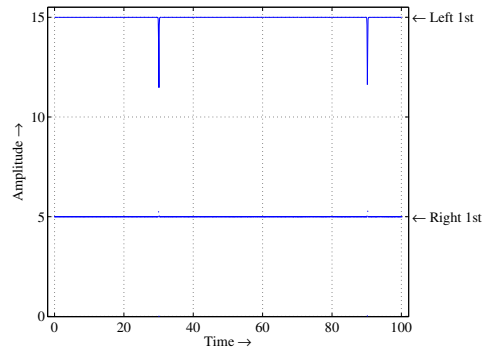
Figure 59: Interactions of KdV solitons. Wave-profile maxima against time in case $\alpha_1 = \alpha_2 = 0.03$, $\beta = 0.0111$, $A_1 = 15$, $A_2 = 5$

5.4 Interactions of KdV soliton ensembles

In Section 4, we found that it is quite conditional to distinguish between the second and the third solution types, i.e., between a KdV soliton ensemble and a KdV soliton ensemble with a weak tail. The tail is sometimes so weak that it is practically indistinguishable by means of wave-profile extrema as well as spectral quantities. For this reason we consider here these two solution types together. In this
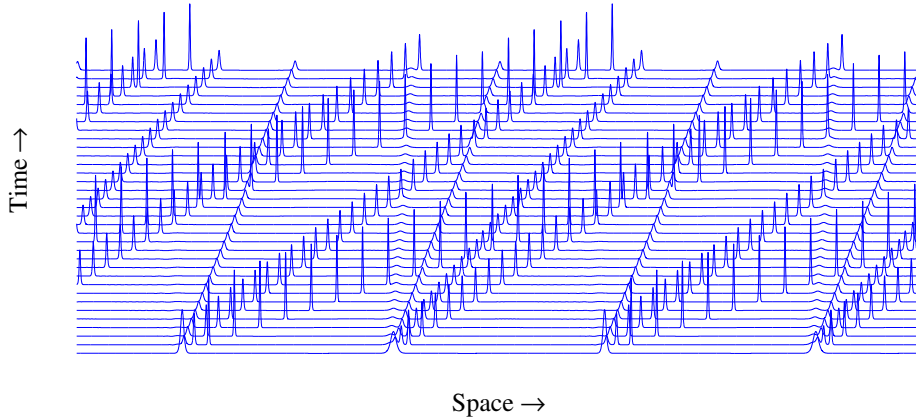
Figure 60: Interactions of KdV soliton ensembles with weak tails. Timeslice plot over two space periods for $\alpha_1 = 1$, $\alpha_2 = 0.1$, $\beta = 111.11$, $A_1 = 8$, $A_2 = 4$
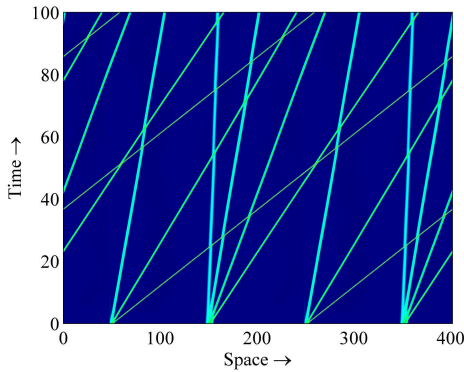
Figure 61: Interactions of KdV soliton ensembles with weak tails. Pseudocolour plot over two space periods for $\alpha_1 = 1$, $\alpha_2 = 0.1$, $\beta = 111.11$, $A_1 = 8$, $A_2 = 4$
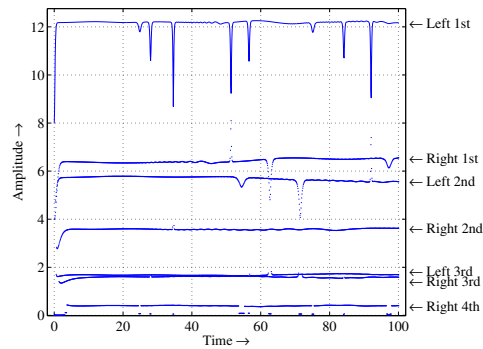
Figure 62: Interactions of KdV soliton ensembles with weak tails. Wave-profile maxima against time in case $\alpha_1 = 1$, $\alpha_2 = 0.1$, $\beta = 111.11$, $A_1 = 8$, $A_2 = 4$

Subsection we consider two sets of initial pulses: in the first case $A_1 = 8$ and $A_2 = 4$ ($\alpha_1 = 1$, $\alpha_2 = 0.1$, $\beta = 111.11$, see Figs. 60–62) and in the second case $A_1 = 15$ and $A_2 = 5$ ($\alpha_1 = 0.07$, $\alpha_2 = 0.03$, $\beta = 111.11$, see Figs. 63–65). In both cases two different soliton ensembles and (very) weak tails emerge from dual sech^2-type initial conditions (59). The number of solitons in the KdV soliton ensemble depends on

the values of dispersion parameters α_1, α_2 and microstructure parameter β and on the value of the amplitude of the pulse A. In the first case an ensemble of three solitons emerges from the left hand side initial pulse and an ensemble of four solitons forms the right hand side pulse. In the second case the number of solitons in both ensembles is two. Emerged soliton ensembles are typical KdV soliton ensembles, i.e., the amplitude of the highest soliton in the KdV ensemble is always higher than the amplitude of the initial pulse. The tail is weak as it does not have a strong influence on the behaviour of the KdV ensemble — it does not change the speed of solitons (see pseudocolour plots in Figs. 61 and 64), but it causes small oscillations in soliton amplitude curves (see Figs. 62 and 65). Solitons with differ-
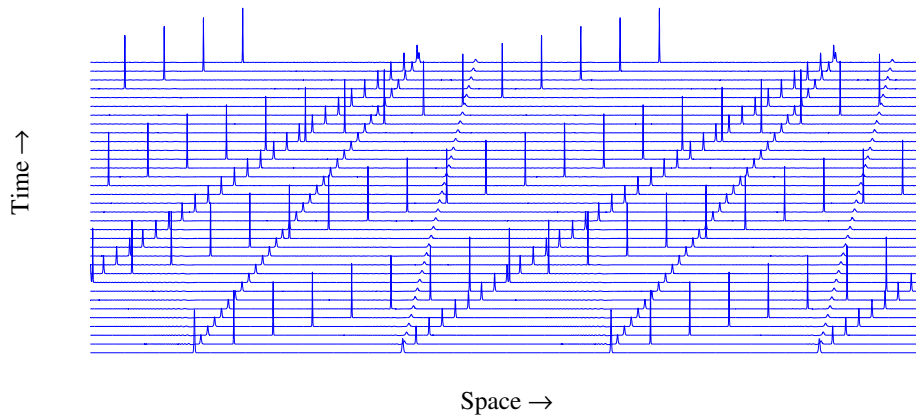
Figure 63: Interactions of KdV soliton ensembles with weak tails. Timeslice plot over two space periods for $\alpha_1 = 0.07$, $\alpha_2 = 0.03$, $\beta = 111.11$, $A_1 = 15$, $A_2 = 5$
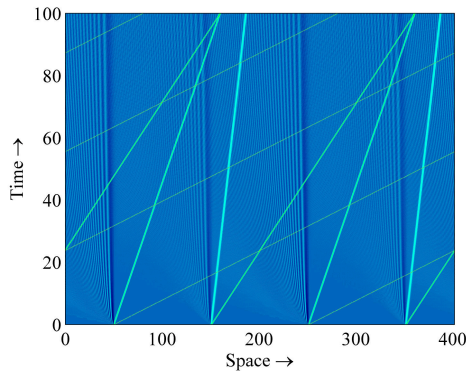
Figure 64: Interactions of KdV soliton ensembles with weak tails. Pseudocolour plot over two space periods for $\alpha_1 = 0.07$, $\alpha_2 = 0.03$, $\beta = 111.1$, $A_1 = 15$, $A_2 = 5$
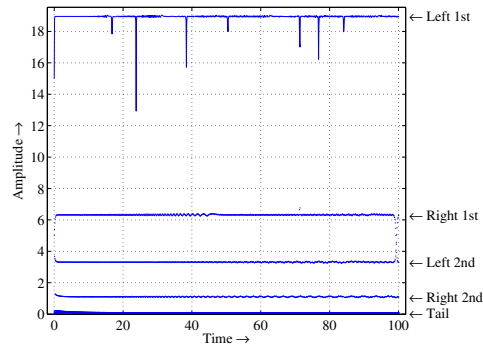
Figure 65: Interactions of KdV soliton ensembles with weak tails. Wave-profile maxima against time in case $\alpha_1 = 0.07$, $\alpha_2 = 0.03$, $\beta = 111.11$, $A_1 = 15$, $A_2 = 5$

ent amplitudes propagate at different speeds and therefore interactions between

emerging solitons take place. One can trace here two types of interactions: (i) between solitons from different ensembles, and (ii) between solitons from the same ensemble. Both interaction types can be characterised as follows: (i) during interactions solitons are phase-shifted (Figs. 61 and 64) and amplitudes of higher solitons decrease (Figs. 62 and 65); (ii) after interactions solitons almost restore their amplitudes (Figs. 62 and 65) and speeds (Figs. 61 and 64). Besides the soliton-soliton interactions all solitons interact with tails. However, as the tails are weak, they do not influence the behaviour of solitons essentially and their influence can be traced only in the curves of wave-profile maxima, where tails can cause small oscillations. In conclusion, one can declare that observed interactions are nearly elastic and therefore the solution can be called solitonic.

5.5 Interactions of solitons with strong tails

In the present case two solitons and strong tails emerge from the initial wave (59) (cf. the fourth solution type in Section 4). Due to different initial amplitudes the solitons emerged propagate at different speeds and therefore interact (see Figs. 66–68). For this solution type the tail is considered to be strong, because it influences the behaviour of the emerged solitary waves essentially: (i) amplitudes of the propagating solitary waves are lower than the amplitudes of the initial ones; (ii) amplitudes of the propagating solitons are not constant, but due to the influence of strong tails they oscillate about a constant level (see Fig. 68). The decrease of the left and the right hand side solitary wave amplitudes is proportional to the initial amplitudes. In the example considered here propagating solitons are approximately 1.4 times lower than the initial waves. The phenomenon of selection takes place, see Section 4 for details. The interaction produces phase shifts in
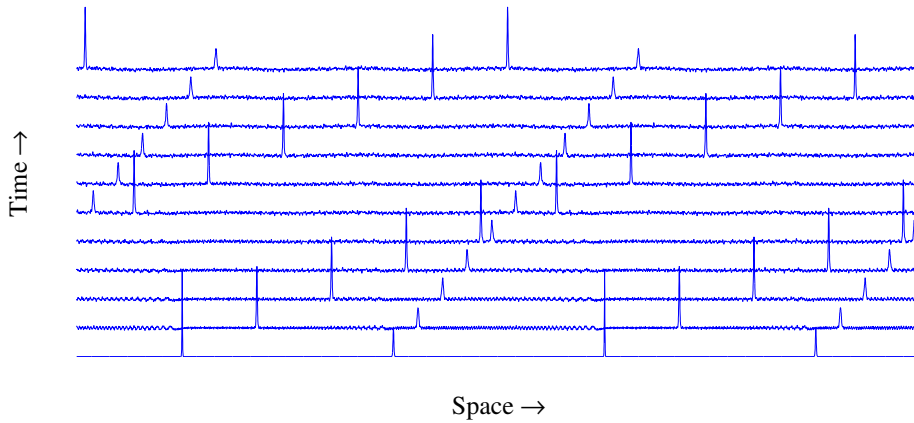
Figure 66: Interactions of solitons with strong tails. Timeslice plot over two space periods for $\alpha_1 = 0.03$, $\alpha_2 = 0.07$, $\beta = 111.11$, $A_1 = 15$, $A_2 = 5$

soliton trajectories — the higher solitary wave is shifted to the right and the lower amplitude solitary wave is shifted to the left. After the interaction both solitons al-

63
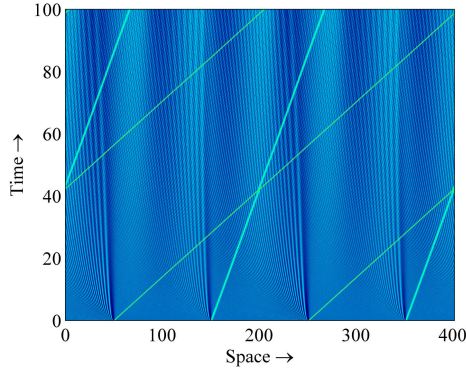
Figure 67: Interactions of solitons with strong tails. Pseudocolour plot over two space periods for $\alpha_1 = 0.03$, $\alpha_2 = 0.07$, $\beta = 111.11$, $A_1 = 15$, $A_2 = 5$

Figure 68: Interactions of solitons with strong tails. Wave-profile maxima against time in case $\alpha_1 = 0.03$, $\alpha_2 = 0.07$, $\beta = 111.11$, $A_1 = 15$, $A_2 = 5$

most restore their amplitudes. Therefore one can say that the interaction is nearly elastic and the usage of the term soliton in Section 4 is verified.

5.6 Interactions of solitary waves with tails and wave packets

The situation discussed in this Subsection corresponds to the fifth solution type in Section 4. In this case solitary waves, tails and wave packets emerge simultaneously. Here we present four examples: in the first case $A_1 = 8$, $A_2 = 4$, $\alpha_1 = 0.05$, $\alpha_2 = 0.11$, and $\beta = 0.0111$ (see Figs. 69–72); in the second case $A_1 = 15$, $A_2 = 5$, $\alpha_1 = 0.05$, $\alpha_2 = 0.03$, and $\beta = 0.111$ (see Figs. 73–76); in the third case $A_1 = 8$, $A_2 = 4$, $\alpha_1 = 0.09$, $\alpha_2 = 0.11$, and $\beta = 0.0111$ (see Figs. 77–80); in the fourth case $A_1 = 12$, $A_2 = 2$, $\alpha_1 = 0.09$, $\alpha_2 = 0.11$, and $\beta = 0.0111$ (see Figs. 81–84). All three components of the solution could be seen in timeslice plots in Figs. 69, 70, 73, 74, 77, 78, 81 and 82.

Due to the complicated structure of the solution, different interactions can take place: (i) solitary wave – solitary wave; (ii) solitary wave – tail; (iii) solitary wave – wave packet; (iv) tail – wave packet; (v) interactions between wave packets.

In Section 4 we found that for all solution types the speed of solitary waves (solitons) depends on the amplitude of the initial wave — the higher the wave the higher its speed. Therefore we expected interacting solitary waves to emerge from different amplitude initial waves for the present solution type. However, due to the emergence of different wave packets the situation here is more complicated than in the case of a single initial pulse. In Section 4 besides the tail and wave packets only one solitary wave emerged. Now several solitary waves can emerge from both initial pulses and interacting solitary waves were detected in few cases only. The influence of different wave packets on the behaviour of solitary waves can be so strong that their amplitudes decrease rapidly and it is practically impossible to distinguish between solitary waves and wave packets in time dependencies of

64

wave-profile maxima. Therefore only time dependencies of global maxima and global minima are presented in Figs. 72, 76, 84 and 80. On the other hand, according to timeslice and pseudocolour plots in Figs. 69–71, 73–75, 77–79 and 81–83 the emerged solitary waves are not completely suppressed. One can say that a very strong selection procedure takes place and shapes of all solitary waves are altered to a certain critical amplitude level, which can be several times lower than the amplitude of the initial wave, see Figs. 72, 76, 80 and 84. In some cases, like the one presented in Figs. 77–80, the selection procedure is not so strong and it is easy to distinguish between solitary waves and wave packets. Due to the fact that all emerged solitary waves are selected to nearly the same amplitude level they all are propagating at nearly the same speed and do not interact, see Figs. 69, 71, 73, 75, 77 and 79. In few cases different solitary waves are selected to different amplitude levels and therefore interactions between solitary waves take place. A corresponding example is presented in Figs. 81–84. However, it is clear that these interactions are not elastic — speeds and amplitudes of solitons and solitary waves are altered during interactions, see Figs. 81–83. Amplitudes of solitary waves oscillate strongly in all four cases due to interactions between solitary waves and wave packets, see Figs. 72, 76, 80 and 84. Notwithstanding these different interactions and the selection phenomenon, all three components of the solution are conserved over the whole integration time interval. In this sense the solution is stable. However, in the present case we cannot declare that emerged solitary waves are solitons because either it is impossible to simulate interactions between solitary waves or interactions are not elastic.
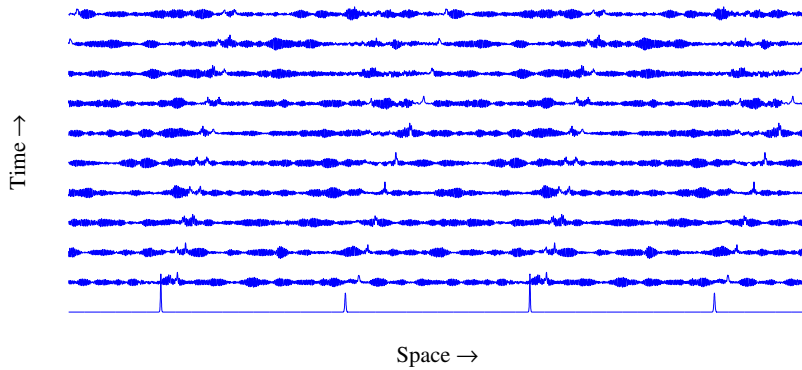
Figure 69: Interactions of solitary waves with tails and wave packets. Timeslice plot over two space periods for $\alpha_1 = 0.05$, $\alpha_2 = 0.11$, $\beta = 0.0111$, $A_1 = 8$, $A_2 = 4$

65
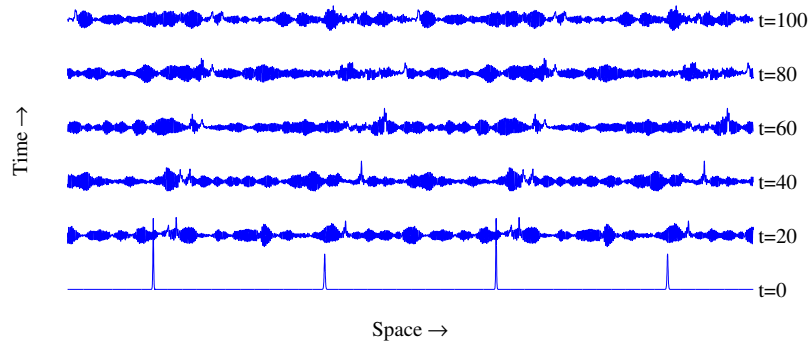
Figure 70: Interactions of solitary waves with tails and wave packets. Single wave-profiles at $t = 0$, $t = 20$, $t = 40$, $t = 60$, $t = 80$, $t = 100$ over two space periods for $\alpha_1 = 0.05$, $\alpha_2 = 0.11$, $\beta = 0.0111$, $A_1 = 8$, $A_2 = 4$
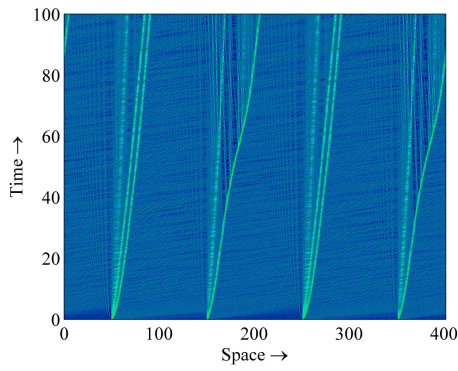
Figure 71: Interactions of solitary waves with tails and wave packets. Pseudocolour plot over two space periods for $\alpha_1 = 0.05$, $\alpha_2 = 0.11$, $\beta = 0.0111$, $A_1 = 8$, $A_2 = 4$
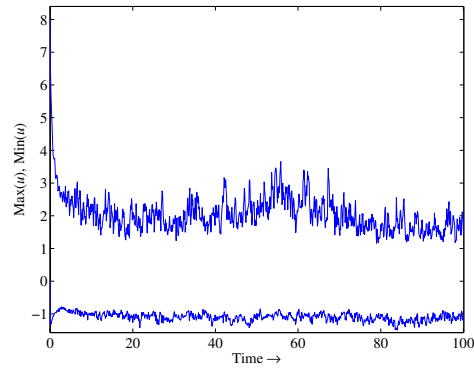
Figure 72: Interactions of solitary waves with tails and wave packets. Wave-profile maximum and minimum against time in case $\alpha_1 = 0.05$, $\alpha_2 = 0.11$, $\beta = 0.0111$, $A_1 = 8$, $A_2 = 4$
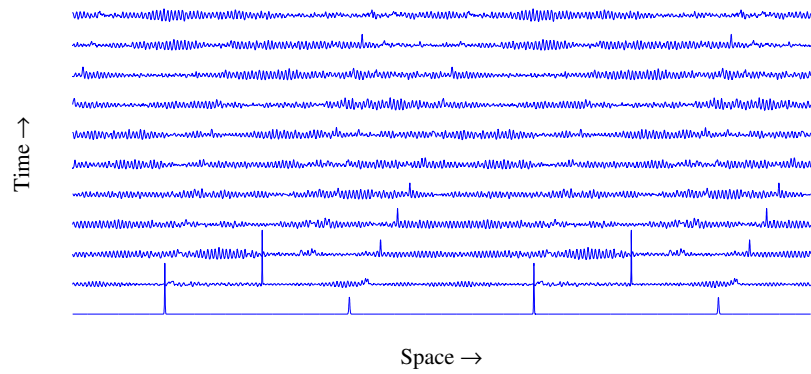
Figure 73: Interactions of solitary waves with tails and wave packets. Timeslice plot over two space periods for $\alpha_1 = 0.05$, $\alpha_2 = 0.03$, $\beta = 0.111$, $A_1 = 15$, $A_2 = 5$
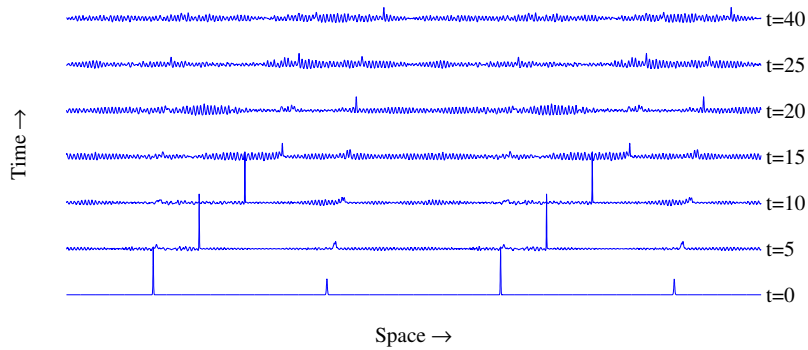
Figure 74: Interactions of solitary waves with tails and wave packets. Single wave-profiles at $t = 0$, $t = 5$, $t = 10$, $t = 15$, $t = 20$, $t = 25$, $t = 40$, over two space periods for $\alpha_1 = 0.05$, $\alpha_2 = 0.03$, $\beta = 0.111$, $A_1 = 15$, $A_2 = 5$
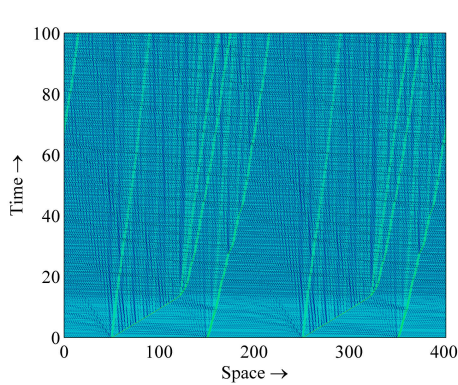
Figure 75: Interactions of solitary waves with tails and wave packets. Pseudocolour plot over two space periods for $\alpha_1 = 0.05$, $\alpha_2 = 0.03$, $\beta = 0.111$, $A_1 = 15$, $A_2 = 5$
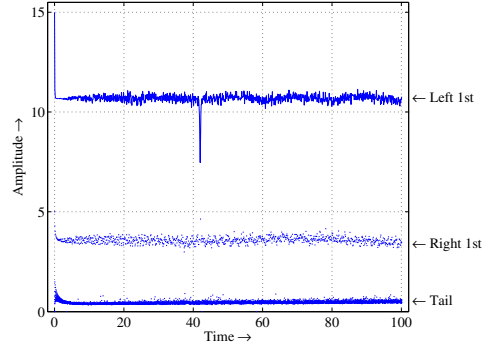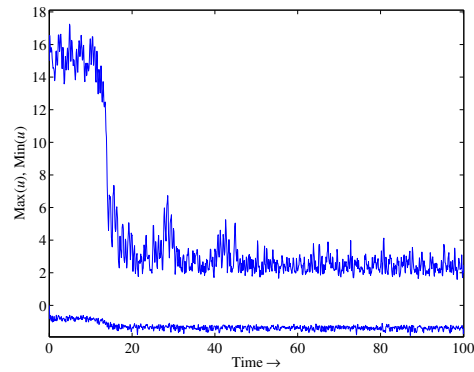

Figure 76: Interactions of solitary waves with tails and wave packets. Wave-profile maximum and minimum against time in case $\alpha_1 = 0.05$, $\alpha_2 = 0.03$, $\beta = 0.111$, $A_1 = 15$, $A_2 = 5$
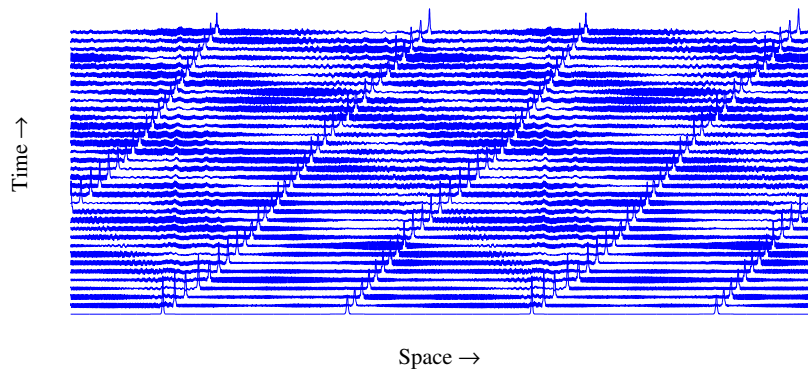
Figure 77: Interactions of solitary waves with tails and wave packets. Timeslice plot over two space periods for $\alpha_1 = 0.09$, $\alpha_2 = 0.11$, $\beta = 0.0111$, $A_1 = 8$, $A_2 = 4$

67
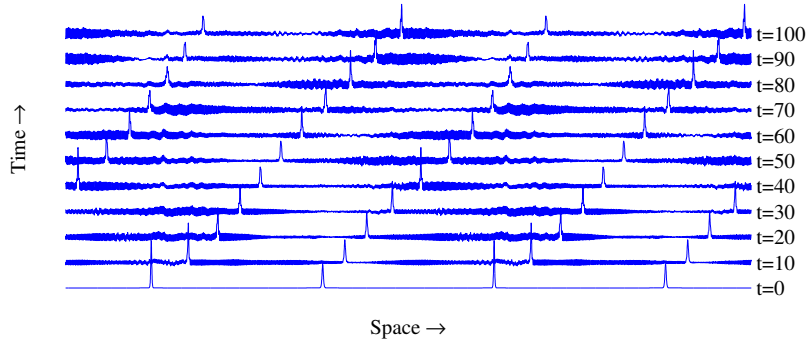
Figure 78: Interactions of solitary waves with tails and wave packets. Single wave-profiles at $t = 0$, $t = 10$, $t = 20$, $t = 30$, $t = 40$, $t = 50$, $t = 60$, $t = 70$, $t = 80$, $t = 90$, $t = 100$ over two space periods for $\alpha_1 = 0.09$, $\alpha_2 = 0.11$, $\beta = 0.0111$, $A_1 = 8$, $A_2 = 4$
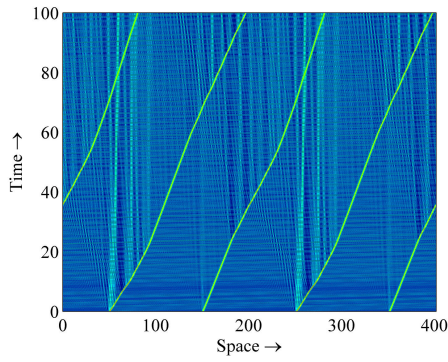
Figure 79: Interactions of solitary waves with tails and wave packets. Pseudo-colour plot over two space periods for $\alpha_1 = 0.09$, $\alpha_2 = 0.11$, $\beta = 0.0111$, $A_1 = 8$, $A_2 = 4$
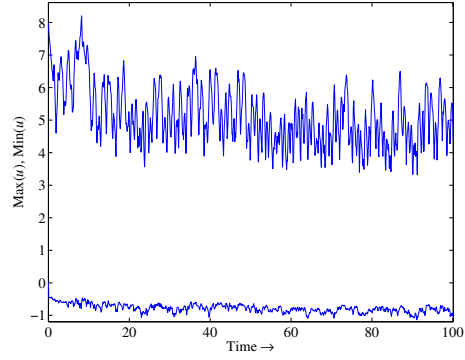
Figure 80: Interactions of solitary waves with tails and wave packets. Wave-profile maximum and minimum against time in case $\alpha_1 = 0.09$, $\alpha_2 = 0.11$, $\beta = 0.0111$, $A_1 = 8$, $A_2 = 4$
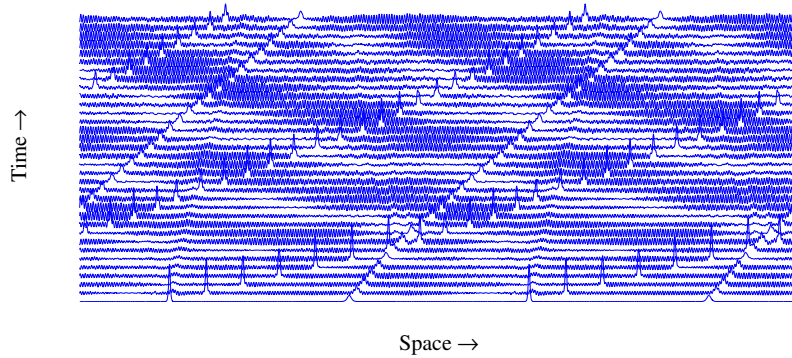
Figure 81: Interactions of solitary waves with tails and wave packets. Timeslice plot over two space periods for $\alpha_1 = 0.09$, $\alpha_2 = 0.11$, $\beta = 0.0111$, $A_1 = 12$, $A_2 = 2$

68
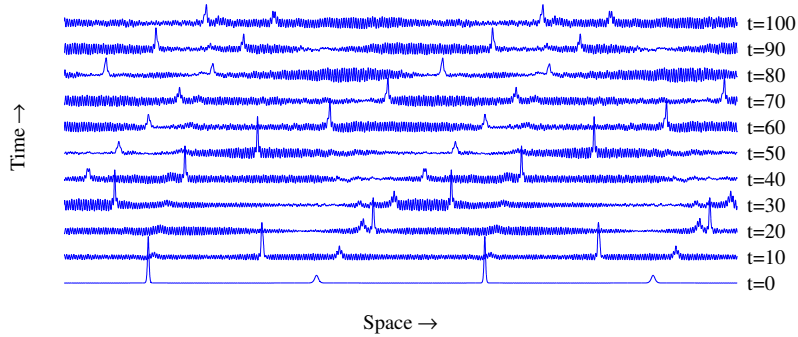
Figure 82: Interactions of solitary waves with tails and wave packets. Single wave-profiles at $t = 0$, $t = 10$, $t = 20$, $t = 30$, $t = 40$, $t = 50$, $t = 60$, $t = 70$, $t = 80$, $t = 90$, $t = 100$ over two space periods for $\alpha_1 = 0.09$, $\alpha_2 = 0.11$, $\beta = 0.0111$, $A_1 = 12$, $A_2 = 2$
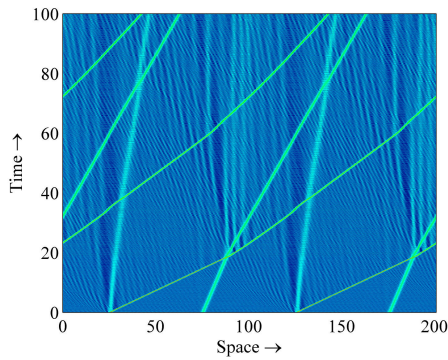
Figure 83: Interactions of solitary waves with tails and wave packets. Pseudo-colour plot over two space periods for $\alpha_1 = 0.09$, $\alpha_2 = 0.11$, $\beta = 0.0111$, $A_1 = 12$, $A_2 = 2$
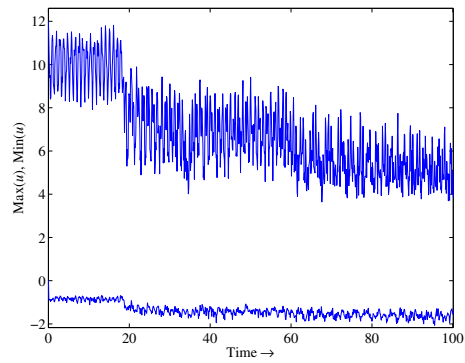
Figure 84: Interactions of solitary waves with tails and wave packets. Wave-profile maximum and minimum against time in case $\alpha_1 = 0.09$, $\alpha_2 = 0.11$, $\beta = 0.0111$, $A_1 = 12$, $A_2 = 2$

69

5.7 Discussion

In Subsection 4.6 we described the phenomenon of wave packet formation in terms of time averaged spectral densities (TANSD). TANSD (58) reflect the contribution of the k-th spectral density over the time interval $[0, t_k]$. Figure 85 presents TANSD for $\alpha_1 = 0.05$, $\alpha_2 = 0.11$, $\beta = 0.0111$, $A_1 = 8$, $A_2 = 4$ and Fig. 86 for $\alpha_1 = 0.05$, $\alpha_2 = 0.03$, $\beta = 0.111$, $A_1 = 15$, $A_2 = 5$ (see the corresponding timeslice plots in Figs. 69 and 73). It is clear that wave packets are formed by amplified higher order
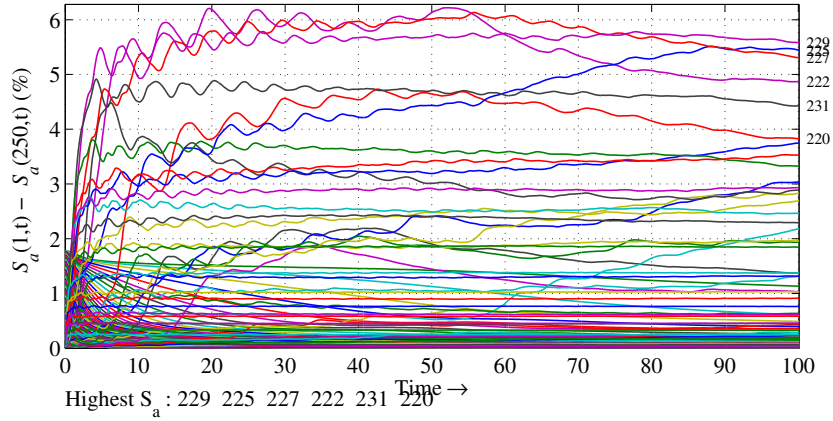
Figure 85: Interactions of solitary waves with tails and wave packets. Time averaged spectral densities plot $\alpha_1 = 0.05$, $\alpha_2 = 0.11$, $\beta = 0.0111$, $A_1 = 8$, $A = 4$
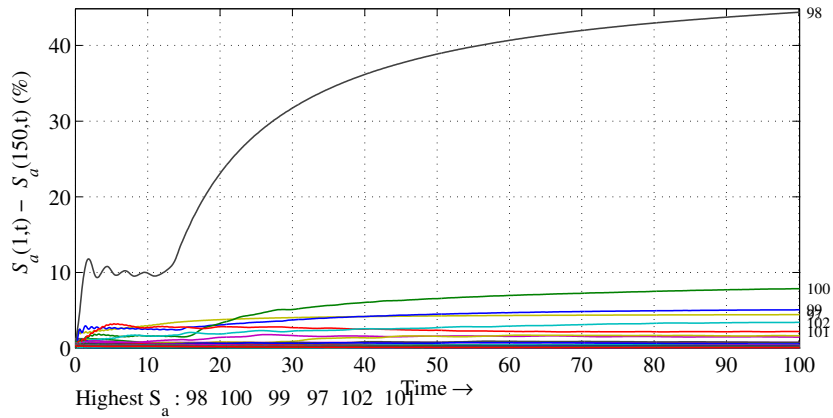
Figure 86: Interactions of solitary waves with tails and wave packets. Time averaged spectral densities plot $\alpha_1 = 0.05$, $\alpha_2 = 0.03$, $\beta = 0.111$, $A_1 = 15$, $A = 5$

harmonics and the highest value of $S_a(k, t)$ determines the number of maxima (oscillations) in the given wave-profile. One can conclude that in Fig. 85 $S_a(k, t)$ for

$218 \leq k \leq 240$ and in Fig. 86 for $97 \leq k \leq 102$ are amplified and therefore generate wave packets.

The wave packets that are formed in the present case are slightly different from the case described in Section 4. In the present case there are two sets of different wave packets, one formed from the left-hand side and the other formed from the right-hand side initial pulse. Based on the analysis in **Publication III** and **Report I** one can say that the shape of the wave packet depends on the amplitude of the initial excitation. In the present case, the number of amplified harmonics is much higher than the number amplified harmonics in the case of single sech^2–type initial condition described in Section 4.

Based on the given examples, it can be concluded, that the wave packets influence the propagation of the solitary waves essentially:

1. In the first (Figs. 69–72) and in the second case (Figs. 73–76) initial solitary waves are decomposed into several solitary waves, which have amplitudes much lower than the amplitudes of the initial waves. In some cases the amplitudes of the emerged solitary waves are so low that it is complicated to distinguish between solitary waves and wave packets in single profiles (Figs. 70 and 74). However, in timeslice plots (Figs. 69 and 73) and pseudocolour plots (Figs. 71 and 75) trajectories of solitary waves can be traced.

2. In the third case, in Figs. 77–80, the amplitude of the higher solitary wave decreases and that of the lower solitary wave increases to a nearly equal level at the beginning of the integration interval. Later the solitary waves change their amplitudes (and speeds) for two times. In other words, between $t \approx 25$ and $t \approx 55$ the right solitary wave is higher than the left one and for $t > 55$ the left solitary wave is again higher and faster. This means that the emerging solitary waves exchange energy between themselves without any "direct" interaction.

3. In the fourth case, in Figs. 81–84, the shape and the speed of the solitary waves are altered during the interaction , i.e., the interaction is not elastic.

In Section 4 the solitonic character was not strictly established for the first, the fourth and the fifth solution types. The analysis presented in the present Section demonstrates that two single KdV solitons (the first solution type in Section 4) interact exactly like solitons in the case of the (classical) KdV equation. Also, numerical simulations demonstrate the solitonic character of the solution of the fourth type (soliton with a strong tail). However, in the case of the fifth solution type (solitary wave with a tail and wave packets), emerged solitary waves do not behave like solitons.

71

6 Conclusions

The term "soliton" has prevailed as a subject for thousands of publications for several decades. Numerous authors have explored and analysed the essence of solitons. Solitons are essential to describe the phenomena such as propagation of some hydrodynamic waves, localised waves in astrophysical plasmas, the propagation of signals in optical fibres, charge transport in conducting polymers, localised modes in magnetic crystals or the dynamics of biological molecules, such as DNA and proteins, etc. Although knowledge collected about the solitons is substantial, there are still wide areas to explore and explain.

The situation with granular materials is similar — numerous scientists are exploring the physics and mathematics provided by granular materials. Models are created and verified and as a result, more exact models are created. Modern technology and efficient numerical algorithms allow us to solve in a short time complex nonintegrable systems that were a main obstacle a couple of years ago.

Models of granular materials exhibit a number of features. One of those features is the coexistence of nonlinearity and dispersion causing the emergence of soliton solution in such kind of media.

In this thesis, the author has studied the problem of one dimensional wave propagation in dilatant granular materials making use of the hierarchical Korteweg–de Vries Eq. (25) (fifth-order nonlinear partial differential equation that includes the mixed derivative). The model equation (25) is integrated numerically under sech^2–type initial conditions in order to simulate emergence, propagation and interactions of solitons and solitary waves.

For numerical integration the discrete Fourier transform based pseudospectral method was used. The accuracy of the numerical simulations was verified by the first and the second conservation law, ensuring a sufficiently high number of space-grid points for numerical integration.

Main results can be summarised as follows:

1. Depending on the character of solutions, four solution types are defined:

    - Single KdV soliton is a soliton solution, because the solitary wave is the analytical soliton solution of the KdV equation that corresponds to both KdV operators in the HKdV Eq. (25). Furthermore, the Single KdV soliton (that propagates at constant speed and shape) interacts elastically with another single KdV soliton. However, the phase-shifts of this solution type coincide with phase shifts of classical KdV solitons.

    - KdV soliton ensemble (with a weak tail) is a soliton solution because a train of elastically interacting solitary waves is formed. The behaviour of the soliton ensemble is very close to that of the KdV. In the considered case the ratios of the amplitudes of solitons practically coincide with the ratios of the amplitude of the classical KdV N–soliton solution. As the initial condition is the soliton solution of the KdV equation

72

which corresponds to the first KdV operator in Eq. (25), then the formation of soliton trains and the tail take place due to the influence of the second KdV operator in Eq. (25).

In Section 4 five solution types were introduced. However, it is quite conditional to distinguish between solution types as 'KdV soliton ensemble' and 'KdV soliton ensemble with a weak tail' on the basis of several numerical experiments. The tail is sometimes so weak that it is practically indistinguishable by means of wave profile extreme as well as spectral quantities. For this reason we consider here these two solution types together.

- Soliton with a strong tail is a soliton solution because the solitary wave (that propagates at constant speed and shape) interacts elastically with another soliton with a strong tail. The formation of the tail is caused by the second KdV operator in Eq. (25).

- Solitary wave with a tail and wave packets — the emerging solitary waves are altered by the wave packets essentially. In some cases it is possible to simulate the interactions but in some it is not. Even if the interactions take place, interactions are not elastic and emerged waves cannot be called solitons. The formation of the tail and wave packet is caused by the second KdV operator in Eq. (25).

2. Dependencies between solution types and material parameters are established. The first solution type appears in case $\alpha_1 = \alpha_2$ for all values of the microstructure parameter β. The second and the third solution type appear for $\alpha_1 > \alpha_2$ in case $\beta = 111.11$ and $\beta = 11.111$ (Fig. 87(a)). The fourth solution type appears for $\alpha_1 < \alpha_2$ in case $\beta = 111.11$ and $\beta = 11.111$ (Fig. 87(b)) and for $\alpha_1 > \alpha_2$ in case $\beta = 0.0111$ (Fig. 87(c)). The fifth solution type can be realised for $\alpha_1 > \alpha_2$ and for $\alpha_1 < \alpha_2$ in case $\beta = 1.111$ and $\beta = 0.111$ (Fig. 87(b)) and for $\alpha_1 < \alpha_2$ in case $\beta = 0.0111$ (Fig. 87(c)). Dispersion parameters have a strong influence on the character of the solution - small changes in the values of parameters may cause changes of the solution type.

3. The influence of the amplitude of the initial solitary wave on the character of the solution was analysed. It was shown that the higher the amplitude of the initial solitary wave the higher the speed of solitons. In the case of the fourth solution type the increase in the initial amplitude causes more complex changes, however, the solution type does not change.

4. Selection phenomenon – the shape of the initial wave is modified in a way to be more appropriate to the actual solution of the equation – appears for the third and fourth solution type.

5. The formation of the wave packets has been explained in terms of TANSD that reflect the influence of higher-order harmonics that dominate over the lower-order harmonics.

73
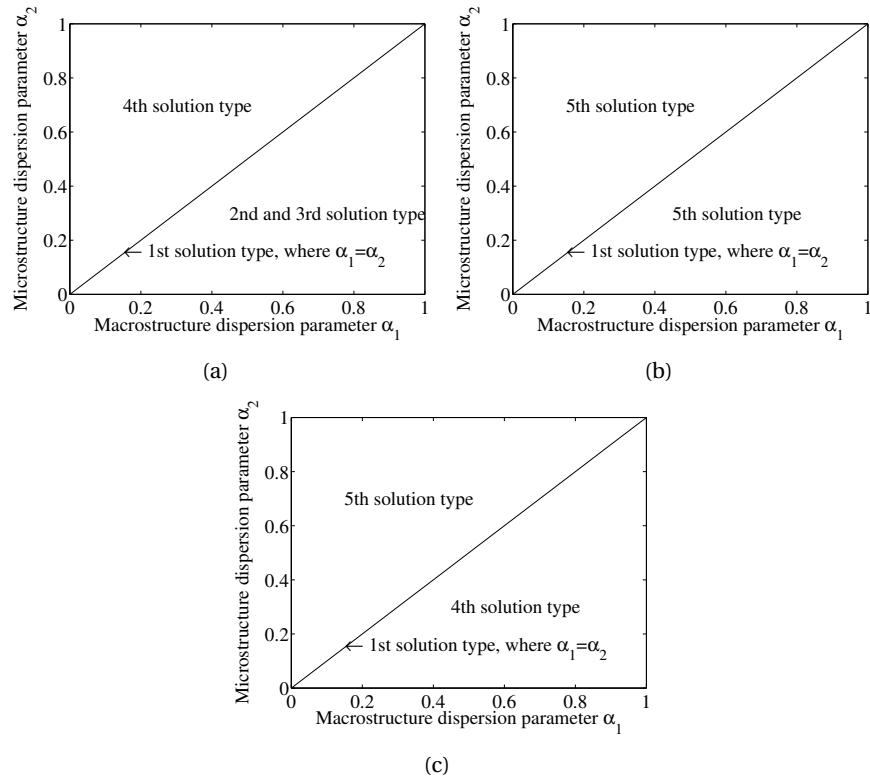
Figure 87: Solution types against dispersion parameters in case $\beta = 111.11$ and $\beta = 11.111$ - (a), $\beta = 1.111$ and $\beta = 0.1111$ - (b), and $\beta = 0.0111$ - (c).

The complicated HKdV (25) model has shown the richness of solutions. The solitonic character of the HKdV (25) model is obvious but in some cases other effects are affecting the emergence of solitons. It is demonstrated that the system tries to keep the fundamental solitonic character, but it is shown what the limits are.

Further studies will be focusing on the simultaneous emergence of solitary waves, the tails and the wave packets in order to deepen the knowledge of this phenomenon. Also, the studies will extend the knowledge on the long-time behaviour of solution types as well as the solutions behaviour in case $\beta < 0$.

Abstract

In this thesis hierarchical Korteweg–de Vries type evolution equation (fifth-order nonlinear partial differential equation that includes the mixed derivative) derived by P. Giovine and F. Oliveri [6] is used to model one dimensional wave propagation in dilatant granular materials. The model equation is integrated numerically under sech^2-type initial conditions using the discrete Fourier transform based pseudospectral method. It is shown that four different solution types can be detected: (i) Single KdV soliton, (ii) KdV soliton ensemble (with a weak tail), (iii) Soliton with a strong tail, (iv) Solitary wave with a tail and wave packets. In the case of first three solution types, one component of the solution is a soliton or an ensemble of solitons. In other words, in these cases emerged solitary waves propagate at constant speed and amplitude and interact elastically. In the case of the fourth solution type, simultaneous emergence of solitary waves, a tail and a wave packet was observed and analysed. Interactions between these solitary waves are not elastic and therefore they cannot be called solitons. The phenomenon of the wave packets is explained in terms of spectral quantities. Main results of the thesis have been presented at eight international conferences and published in five papers of journals and proceedings indexed by ISI Web of Knowledge.

Kokkuvõte

Käesolevas töös uuritakse ühedimensionaalset lainelevi granuleeritud materjalides. Mudelvõrrandiks on hierarhiline Kortewegi–de Vriesi (KdV) tüüpi evolutsioonivõrrand, mis on tuletatud Pasquale Giovine ja Francesco Oliveri poolt [6].

Mudelvõrrand (viiendat järku segaosatuletistega mittelineaarne diferentsiaalvõrrand) on lahendatud numbriliselt kahe lokaliseeritud algtingimuste komplekti ja perioodiliste rajatingimuste korral laias materjaliparameetrite vahemikus (kaks dispersiooni- ja üks mikrostruktuuri parameeter). Esimeseks algtingimuseks on üksik $sech^2$–tüüpi üksiklaine, mis on klassikalise KdV võrrandi analüütiliseks lahendiks. Teiseks algtingimuseks on kaks kõrvuti asetsevat $sech^2$–tüüpi üksiklainet, mis on omavahel nihutatud. Numbriliseks integreerimiseks on kasutatud pseudospektraalmeetodit.

Töös on leitud, et lokaliseeritud alghäiritusest (üksiklainest) võib formeeruda nelja tüüpi lahendeid: (i) üksik KdV soliton, (ii) KdV solitonide ansambel (koos nõrga sabaga), (iii) soliton koos tugeva sabaga, (iv) üksiklaine koos saba ja lainepaketiga. Kolme esimese lahenditüübi korral käituvad formeerunud üksiklained kui solitonid kuid neljanda korral mitte. Töös on esitatud lahendi tüüpide esiletuleku piirkonnad dispersiooniparameetrite tasandil. Lisaks on selgitatud lainepaketi formeerumist ja selle tekkemehhanismi spektraalanalüüsi põhjal.

Käesoleva töö tulemused on esitletud kaheksal rahvusvahelisel konverentsil ja avaldatud viies teadusartiklis rahvusvaheliselt tunnustatud erialaajakirjades ja konverentsikogumikes, mis on indekseeritud ISI Web of Knowledge poolt.

References

[1] T. Dauxois, M. Peyrard, Physics of Solitons, Cambridge University Press, New York, 2006.

[2] N. J. Zabusky, M. D. Kruskal, Interaction of "Solitons" in a collisionless plasma and the recurrence of initial states, Phys. Rev. Lett. 15 (6) (1965) 240–243.

[3] Y. Wang, K. Hutter, Granular Material Theories Revisited, in: N. J. Balmforth, A. Provenzale (Eds.), Geomorphological Fluid Mechanics, Vol. 582 of Lecture Notes in Physics, Berlin Springer Verlag, Springer Berlin / Heidelberg, 2001, pp. 79–107.

[4] M. Massoudi, M. M. Mehrabadi, A continuum model for granular materials: Considerding dilatancy and the Mohr–couloumb criterion, Acta Mechanica 152 (2001) 121–138.

[5] M. A. Goodman, S. C. Cowin, A continuum theory for granular materials, Arch. Rational Mech. Anal. 44 (4) (1972) 249–266.

[6] P. Giovine, F. Oliveri, Dynamics and wave propagation in dilatant granular materials, Meccanica 30 (4) (1995) 341–357.

[7] J. S. Russell, Report on waves, in: Rep. 14th Meet. Bit. Assoc. Adv. Sci., John Murray, London, 1844, pp. 311–392.

[8] M. Remoissenet, Waves Called Solitons: Concepts and Experiments, Springer-Verlag, Berlin, 1994.

[9] G. Eilenberger, Solitons: Mathematical Methods for Physicists, Springer, 1981.

[10] P. G. Drazin, Solitons, Cambridge University Press, Cambridge, 1983.

[11] P. G. Drazin, R. S. Johnson, Solitons: an Introduction, Cambridge University Press, Cambridge et al., 1989.

[12] N. Zabusky, Computational synergetics and mathematical innovation, J. Comp. Phys. 43 (1981) 195–249.

[13] E. Infled, G. Rowlands, Nonlinear Waves, Solitons and Chaos, Cambridge University Press, 1990.

[14] T. Soomere, J. Engelbrecht, Extreme elevations and slopes of interacting Kadomtsev–Petviashvili solitons in shallow water, in: Proc. of a Workshop organized by IFREMER, IFREMER actes de colloques, 2005, pp. 92–101.

[15] T. Soomere, Interaction of Kadomtsev–Petviashvili solitons with unequal amplitudes, Phys. Lett. A 332 (1-2) (2004) 74–81.

[16] T. Soomere, J. Engelbrecht, Weakly two-dimensional interaction of solitons in shallow water, Eur. J. Mech. B. Fluids 25 (2006) 636–648.

[17] R. A. Meyers (Ed.), Encyclopedia of Complexity and Systems Science, Springer, 2009.

[18] M. Ablowitz, P. Clarkson, Solitons, Nonlinear Evolution Equations and Inverse Scattering, Cambridge University Press, Cambridge, 1991.

[19] J. Hunter, J. Scheurle, Existence of perturbed solitary wave solutions to a model equation for water waves, Phys. D 32 (2) (1988) 253 – 268.

[20] T. Kakutani, H. Ono, Weak non-linear hydromagnetic waves in a cold collision-free plasma, J. Phys. Soc. Jpn. 26 (5) (1969) 1305–1318.

[21] V. I. Karpman, J. M. Vanden-Broeck, Stationary solitons and stabilization of the collapse described by KdV-type equations with high nonlinearities and dispersion, Phys. Lett. A 200 (6) (1995) 423 – 428.

[22] S. Kawamoto, Solitary wave solutions of the Korteweg–de Vries equation with higher order nonlinearity, J. Phys. Soc. Jpn. 53 (11) (1984) 3729–3731.

[23] A. Porubov, G. Maugin, V. Gursky, V. Krzhizhanovskaya, On some localized waves described by the extended KdV equation, C. R. Mecanique 333 (7) (2005) 528–533.

[24] A. V. Porubov, Amplification of Nonlinear Strain Waves in Solids, World Scientific, Singapore, 2003.

[25] O. Ilison, A. Salupere, Propagation of sech^2-type solitary waves in higher-order KdV-type systems, Chaos Solitons Fractals 26 (2) (2005) 453 – 465.

[26] O. Ilison, A. Salupere, On the propagation of solitary pulses in microstructured materials, Chaos Solitons Fractals 29 (1) (2006) 202 – 214.

[27] A. Salupere, G. Maugin, J. Engelbrecht, Solitons in systems with a quartic potential and higher–order dispersion, Proc. Estonian Acad. Sci. Phys. Math. 46 (1997) 118–127.

[28] T. R. Marchant, Undular bores and the initial-boundary value problem for the modified Korteweg–de Vries equation, Wave Motion 45 (4) (2008) 540–555.

[29] P. Peterson, E. van Groesen, A direct and inverse problem for wave crests modelled by interactions of two solitons, Phys. D 141 (3-4) (2000) 316–332.

[30] Y. Tan, J. Yang, D. Pelinovsky, Semi-stability of embedded solitons in the general fifth-order KdV equation, Wave Motion 36 (3) (2002) 241–255.

[31] A. Ludu, Solitons and antisolitons on bounded surfaces, Math. Comput. Simulation 69 (2005) 389–399.

[32] A. Ludu, P. Kevrekidis, Nonlinear dispersion relations, Math. Comput. Simulation 74 (2007) 229–236.

[33] J. Guo, T. Taha, Parallel implementation of the split-step and the pseudospectral methods for solving higher KdV equation, Math. Comput. Simulation 62 (1-2) (2003) 41–51.

[34] E. Pelinovsky, A. Sergeeva (Kokorina), Numerical modeling of the KdV random wave field, Eur. J. Mech. B Fluids 25 (4) (2006) 425–434.

[35] O. Reynolds, On the dilatancy of media composed of rigid particles in contact with experimental illustrations, in: Papers on Mechanical and Physical Subjects, Vol. 2, Cambridge University Press, 1901, pp. 203–216.

[36] O. Reynolds, Experiments showing dilatancy, a property of granular material, possibly connected with gravitation, in: Papers on Mechanical and Physical Subjects, Vol. 2, Cambridge University Press, 1901, pp. 217–227.

[37] C. Godano, F. Oliveri, Nonlinear seismic waves: a model for site effects, Int. J. Non Linear Mech. 34 (3) (1998) 457 – 468.

[38] S. C. Cowin, A theory for the flow of granular materials, Powder Tech. 9 (2-3) (1974) 61 – 69.

[39] C. Fang, Y. Wang, K. Hutter, A thermo-mechanical continuum theory with internal length for cohesionless granular materials - Part I. A class of constitutive models, Contin. Mech. Thermodyn. 17 (8) (2006) 545–576.

[40] P. Giovine, An Extended Continuum Theory for Granular Media, Vol. 1937 of Lecture Notes in Math., Springer, Berlin, 2008.

[41] A. Bedford, D. Drumheller, On volume fraction theories for discretized materials, Acta Mechanica 48 (1983) 173–184.

[42] G. Whitham, Linear and Nonlinear Waves, John Wiley & Sons, 1974.

[43] L. Ilison, Waves in granular materials and dispersion analysis, Bachelor's thesis, Tallinn University of Technology (2001).

[44] L. Ilison, A. Salupere, Solitons in hierarchical Korteweg–de Vries type systems, Research Report Mech 240/02, Institute of Cybernetics at Tallinn University of Technology (2002).

[45] L. Ilison, Soliton-type waves in granular materials, Master's thesis, Tallinn University of Technology (2003).

[46] A. Salupere, On the application of the pseudospectral method for solving the Korteweg–de Vries equation, Proc. Estonian Acad. Sci. Phys. Math. 44 (1) (1995) 73–87.

[47] A. Salupere, On the application of pseudospectral methods for solving non-linear evolution equations, and discrete spectral analysis, in: Proc. of 10th Nordic Seminar on Computational Mechanics, Tallinn University of Technology, Tallinn, 1997, pp. 76–83.

[48] B. Fornberg, A Practical Guide to Pseudospectral Methods, Cambridge University Press, Cambridge, 1998.

[49] H.-O. Kreiss, J. Oliger, Comparison of accurate methods for the integration of hyperbolic equations, Tellus 30 (1972) 341–357.

[50] E. Jones, T. Oliphant, P. Peterson, SciPy: Open source scientific tools for Python, http://www.scipy.org (2007).

[51] M. Frigo, S. Johnson, The design and implementation of FFTW3, in: Proceedings of the IEEE, Vol. 93, Ieee-Inst Electrical Electronics Engineering Inc., 2005, pp. 216–231.

[52] P. Peterson, F2PY: Fortran to Python interface generator, http://cens.ioc.ee/projects/f2py2e/ (2005).

[53] A. C. Hindmarsh, ODEPACK, a systematized collection of ODE solvers, in: R. S. Stepleman, et al. (Eds.), Scientific Computing, North-Holland, Amsterdam, 1983, pp. 55–64.

[54] C. Christov, M. Velarde, Dissipative solitons, Phys. D 86 (1995) 323–347.

[55] I. Kliakhandler, A. Porubov, M. Velarde, Localized finite-amplitude disturbances and selection of solitary waves, Phys. Rev. E 62 (4) (2000) 4959–4962.

[56] A. V. Porubov, V. V. Gursky, G. A. Maugin, Selection of localized nonlinear seismic waves, Proc. Estonian Acad. Sci. Phys. Math. 52 (1) (2003) 85–93.

[57] L. Galgani, A. Giorgilli, A. Martinoli, S. Vanzini, On the problem of energy equipartition for large systems of the Fermi-Pasta-Ulam type: analytical and numerical estimates, Phys. D 59 (4) (1992-4) 334–348.

[58] J. Billingham, A. King, Wave Motion, Cambridge University Press, 2000.

[59] L. Ilison, A. Salupere, Solitons in hierarchical Korteweg–de Vries type systems, Proc. Estonian Acad. Sci. Phys. Math. 52 (1) (2003) 135–144.

[60] J. Fujioka, A. Espinosa-Ceron, R. Rodriguez, A survey of embedded solitons, in: Rev. Mex. Fis., Vol. 52, Sociedad mexicana de física, Mexico, 2006, pp. 6–14.

[61] J. Yang, B. A. Malomed, D. J. Kaup, Embedded solitons in second-harmonic-generating systems, Phys. Rev. Lett. 83 (10) (1999) 1958–1961.

[62] J. Yang, B. A. Malomed, D. J. Kaup, A. R. Champneys, Embedded solitons: a new type of solitary wave, Math. Comput. Simulation 56 (2001) 585–600.

[63] W. I. Newman, D. K. Campbell, J. M. Hyman, Identifying coherent structures in nonlinear wave propagation, Chaos 1 (1991) 77–94.

[64] A. Salupere, P. Peterson, J. Engelbrecht, Long-time behaviour of soliton ensembles. Part I—Emergence of ensembles, Chaos Solitons Fractals 14 (2002) 1413 – 1424.

PUBLICATIONS

Publication I

Lauri Ilison, Andrus Salupere and Pearu Peterson, *On the propagation of localized perturbations in media with microstructure*

Publication II

Andrus Salupere, **Lauri Ilison**, and Kert Tamm. *On numerical simulation of propagation of solitons in microstructured media*

Publication III

Lauri Ilison and Andrus Salupere, *Propagation of* sech^2*–type solitary waves in hierarchical KdV-type systems*

Publication IV

Andrus Salupere and **Lauri Ilison**, *Numerical simulation of interaction of solitons and solitary waves in granular materials*

The paper has been accepted for publishing in Proceedings of EUROMECH - MECAMAT conference, Mechanics in microstructured solids: cellular materials, fibre reinforced solids and soft tissues, Lecture Notes in Applied and Computational Mechanics, 8 pp., Springer, 2009.

Publication V

Lauri Ilison and Andrus Salupere, *Numerical simulation of interaction of solitons and solitary waves in hierarchical KdV-type systems*

Curriculum Vitae

1. Personal data

Name	Lauri Ilison
Date and place of birth	26.12.1978, Tallinn
Citizenship	Estonia
Marital status	cohabitation
Children	2 sons (4 and 2 years old)

2. Contact Information

Address	Akadeemia tee 21, 12618, Tallinn
Phone	(+372) 5 111 003
E-mail	lauri@cens.ioc.ee

3. Education

Education institution	Graduation year	Education (filed of study, degree)
Tallinn University of Technology	2001	Engineering physics / BSc
Tallinn University of Technology	2003	Engineering physics / MSc

4. Language competence/skills (fluent, average or basic skills)

Language	Level
Estonian	fluent
English	fluent
Russian	average

5. Special cources

Period	Educational or other organisation
September, 6–10th 2004	CISM'i course: "Surface waves in Geomechanics: Direct and Inverse modelling for Soils and Rock", Udine, Italy

6. Professional employment

Period	Organisation	Position
2001 – to date	Institute of Cybernetics, Tallinn University of Technology	Researcher
2000 – 2002	Sampo Pank AS	Project manager
2002 – 2004	Sampo Pank AS	Head of E-banking
2004 – 2007	Sampo Pank AS	Head of Electronic banking department
2007 – to date	Danske Bank A/S Estonian Branch	Head of Channels

7. Awards

   - Scholarship awarded by Union of Alumni of Tallinn University of Technology, 1999
   - Estonian Academy of Sciences - Student's Research Award, 2003

8. Results in sport

   - Estonian Junior Champion - 16 times in Underwater Orienteering and Finswimming during 1993–1995
   - Estonian Champion - 22 times in Underwater Orienteering and Finswimming during 1994–1999
   - Absolute champion of Estonia in Underwater Orienteering 1996 and 1998
   - The best sportsman in Underwater Orienteering in Estonia - 1995, 1996 and 1997
   - World Championship - SILVER medal - Underwater Orienteering, Otepää, Estonia, 1996
   - European Championship - GOLD medal - Underwater Orienteering, Seĉ, Czech Republic, 1997
   - World Championship - BRONZE medal - Underwater Orienteering, Budapest, Hungary, 1998

9. Defended theses

   - Waves in granular materials and dispersion analysis, BSc, Tallinn University of Technology, 2001
   - Soliton-type waves in granular materials, MSc, Tallinn University of Technology, 2003

10. Main areas of scientific work / current research topics
    Nonlinear waves in microstructured solids (granular materials), solitons

11. Scientific work

   Papers

   I. Lauri Ilison and Andrus Salupere. On solitons in dilatant granular materials. In E. Lund, N. Olhoff, and J. Stegman, editors, *Proc. 15th Nordic Seminar on Computational Mechanics, 18–19 October, 2002 Aalborg*, pages 181–184, 2002.

   II. Lauri Ilison and Andrus Salupere. Solitons in hierarchical Korteweg–de Vries type systems. *Proc. Estonian Acad. Sci. Phys. Math.*, 52(1):125–134, 2003. (special issue: Proc. of the EUROMECH Colloquium 436 "Nonlinear Waves in Microstructured Solids", Tallinn, 2002).

III. Andrus Salupere, Jüri Engelbrecht, Olari Ilison, and Lauri Ilison. On solitons in microstructured solids and granular materials. *Math. Comput. Simulation*, 69:502–513, 2005.

IV. Lauri Ilison, Andrus Salupere, and Pearu Peterson. On the propagation of localised perturbations in media with microstructure. *Proc. Estonian Acad. Sci. Phys. Math.*, 56(2):84–92, 2007, (special issue: Proc. of the EUROMECH Colloquium 478 "Non-equilibrium Dynamical Phenomena in Inhomogeneous Solids", Tallinn, 2006).

V. Andrus Salupere, Lauri Ilison, and Kert Tamm. On numerical simulation of propagation of solitons in microstructured media. In Michail D. Todorov, editor, *Proceedings of the 34th Conference on Applications of Mathematics in Engineering and Economics (AMEE '08)*, volume 1067 of Aip Conference Proceedings, 155–165. American Institute of Physics, 2008.

VI. Lauri Ilison and Andrus Salupere. Propagation of $sech^2$–type solitary waves in hierarchical KdV–type systems. *Math. Comput. Simulation*, 20 pp., 2009. (accepted).

VII. Andrus Salupere and Lauri Ilison. Numerical simulation of interaction of solitons and solitary waves in granular materials. In J.F. Ganghoffer and Franco Pastrone, editors, *Proceedings of EUROMECH-MECAMAT conference, Mechanics in microstructured solids: cellular materials, fibre reinforced solids and soft tissues, Lect. Notes Appl. Comput. Mech.*, 8 pp., Springer, 2009. (accepted).

VIII. Lauri Ilison and Andrus Salupere. Numerical simulation of interaction of solitons and solitary waves in hierarchical KdV-type systems. *Commun. Nonlinear Sci. Numer. Simul.*, 10 pp., 2009. (submitted).

Abstracts

I. Lauri Ilison and Andrus Salupere. Solitons in hierarchical Korteweg-de Vries type systems. In Gérard A. Maugin and Jüri Engelbrecht, editors, *EUROMECH 436, Nonlinear Waves in Microstructured Solids, May 29– June 01, 2002, Tallinn, Estonia, Book of Abstracts*, page 28, 2002.

II. Andrus Salupere, Jüri Engelbrecht, Lauri Ilison, and Martti Kukk. Emergence of soliton ensembles from KdV-like systems. In J. Starke and J. Vollmer, editors, *Dynamics Days Europe, Heidelberg, July 15–19, 2002, Book of Abstracts*, page 82, 2002.

III. Andrus Salupere, Jüri Engelbrecht, Olari Ilison, and Lauri Ilison. On solitons in microstructured solids and granular materials. In T.R. Taha, editor, *The Third International Conference on Nonlinear Evolution Equations and Wave Phenomena: Computation and Theory, April 7–10, 2003, The University of Georgia, Athens, Book of Abstracts*, page 171, 2003.

IV. Andrus Salupere, Jüri Engelbrecht, Lauri Ilison, and Kert Tamm. On solitary waves and solitons in hierarchical systems. In T.R. Taha, editor, *The Forth International Conference on Nonlinear Evolution Equations and Wave Phenomena: Computation and Theory, April 10–14, 2005, The University of Georgia, Athens, Book of Abstracts*, page 158, 2005.

V. Andrus Salupere, Jüri Engelbrecht, Olari Ilison, and Lauri Ilison. Propagation of solitary waves in microstructured media. In *Abstract Book, FUDoM 2005, Finno–Ugric International Conference of Mechanics with ESI Group Symposium, 29 May–4 June, 2005, Ráckeve/Budapest, Hungary*, 2005. 1p.

VI. Andrus Salupere, Jüri Engelbrecht, Olari Ilison, and Lauri Ilison. Solitary waves governed by complicated nonlinearity and dispersion. In *Abstract Book, FPU+50: Nonlinear Waves 50 Years After Fermi-Pasta-Ulam. 21–25 June, 2005, INSA de Rouen, France*, pages 16–17, 2005.

VII. Andrus Salupere, Jüri Engelbrecht, Olari Ilison, and Lauri Ilison. On solitary waves and solitons in microstructured media. In *Abstract Book, RANM 2005, Recent Advances in Nonlinear Mechanics, 30 Aug–1 Sept 2005, University of Aberdeen, Scotland*, UK, page 144, 2005.

VIII. Lauri Ilison and Andrus Salupere. On the propagation of localised perturbations in continua with microstructure. In *EUROMECH Colloquium 478, Non-equilibrium Dynamical Phenomena in Inhomogeneous Solids, 13–16 June, 2006, Tallinn, Book of Abstracts*, page 20, 2006.

IX. Lauri Ilison and Andrus Salupere. On the formation and interaction of solitons and solitary waves in granular media. In *Book of Abstracts, 27th Dynamics Days Europe, Loughborough, 9–13 July 2007, Loughborough University*, page 120, 2007.

X. Andrus Salupere and Lauri Ilison. Numerical simulation of interaction of solitons and solitary waves in granular materials. In *11th EUROMECH-MECAMAT Conference "Mechanics of microstructured solids: cellular materials, fibre reinforced solids and soft tissues", Torino, Italy, 10–14 March, 2008, Book of Abstracts*, Torino, 2008, page 59, 2008.

XI. Andrus Salupere and Lauri Ilison. *On interaction of solitary waves in granular materials.* 7th EUROMECH Solid Mechanics Conference (ESMC 2009), Lisbon, Portugal, 7–11. Sept., 2009. (accepted)

Conference presentations

I. Lauri Ilison and Andrus Salupere. *Solitons in hierarchical Korteweg-de Vries type systems.* EUROMECH 436, Nonlinear Waves in Microstructured Solids, May 29–June 01, 2002, Tallinn, Estonia.

II. Jüri Engelbrecht, Andrus Salupere, Pearu Peterson, Olari Ilison, and Lauri Ilison. Modified KdV-type equations and solitary waves. *Workshop "Dynamical System Methods in Nonlinear Evolution Equations"*, 4–5 July, 2002, Loughborough, UK.

III. Andrus Salupere, Jüri Engelbrecht, Lauri Ilison, and Martti Kukk. *Emergence of Soliton Ensembles from KdV-like Systems.* Dynamics Days Europe, 15–19 July, 2002, Heidelberg, Germany.

IV. Lauri Ilison and Andrus Salupere. *Solitons in hierarchical Korteweg-de Vries type systems.* 11th Estonian Days of Mechanics, 12–13. Sept., 2002, Tallinn, Estonia.

V. Lauri Ilison and Andrus Salupere. *On solitons in dilatant granular materials.* 15th Nordic Seminar on Computational Mechanics, 18–19 Oct., 2002, Aalborg, Denmark.

VI. Andrus Salupere, Olari Ilison, Lauri Ilison, and Jüri Engelbrecht. *On Solitons in Microstructured Solids and Granular Materials.* The Third International Conference on Nonlinear Evolution Equations and Wave Phenomena: Computation and Theory, 7–10 April, 2003, The University of Georgia, Athens, USA.

VII. Andrus Salupere, Jüri Engelbrecht, Lauri Ilison, and Kert Tamm. *On Solitary Waves and Solitons in Hierarchical Systems.* IMACS 2005, The Forth International Conference on Nonlinear Evolution Equations and Wave Phenomena: Computation and Theory, 10–14 April, 2005, The University of Georgia, Athens, USA.

VIII. Andrus Salupere, Jüri Engelbrecht, Olari Ilison, and Lauri Ilison. *Propagation of Solitary Waves in Microstructured Media.* FUDoM 2005, Finno-Ugric International Conference of Mechanics with ESI Group Symposium, 29 May–4 June, 2005, Ráckeve (Budapest), Hungary.

IX. Andrus Salupere, Jüri Engelbrecht, Olari Ilison, and Lauri Ilison. *Solitary Waves Governed by Complicated Nonlinearity and Dispersion.* FPU +50: Nonlinear Waves 50 Years After Fermi-Pasta-Ulam. 21–25 June, 2005, INSA de Rouen, France.

X. Andrus Salupere, Jüri Engelbrecht, Olari Ilison, and Lauri Ilison. *On Solitary Waves and Solitons in Microstructured Media.* RANM 2005, Resent Advances in Nonlinear Mechanics, 30 Aug–1 Sept, 2005, University of Aberdeen, Scotland, UK.

XI. Lauri Ilison and Andrus Salupere. *On the propagation of localised perturbations in continua with microstructure.* EUROMECH Colloquium 478, Non-equilibrium Dynamical Phenomena in Inhomogeneous Solids, 13–16 June, 2006, Tallinn, Estonia.

XII. Lauri Ilison and Andrus Salupere. *On the formation and interaction of solitons and solitary waves in granular media.* Dynamics Days Europe 2007, Loughborough University, UK, 9–13 July, 2007.

XIII. Andrus Salupere and Lauri Ilison. *Numerical simulation of interaction of solitons and solitary waves in granular materials.* 11th EUROMECH-MECAMAT Conference "Mechanics of microstructured solids: cellular

materials, fibre reinforced solids and soft tissues", Torino, Italy, 10–14 March, 2008.

XIV. Lauri Ilison and Andrus Salupere. *Solitons and solitary waves in granular materials.* 11th Estonian Days of Mechanics, 15–16. Sept., 2008, Tallinn, Estonia.

XV. Andrus Salupere and Lauri Ilison. *On interaction of solitary waves in granular materials.* 7th EUROMECH Solid Mechanics Conference (ESMC2009), Lisbon, Portugal, 7–11. Sept., 2009. (submitted)

Research reports

I. Lauri Ilison and Andrus Salupere. Solitons in hierarchical Korteweg-de Vries type systems. Research Report Mech 240/02, Institute of Cybernetics at Tallinn Technical University, 2002.

II. Lauri Ilison and Andrus Salupere. Propagation of localised perturbations in granular materials. Research Report Mech 287/07, Institute of Cybernetics at Tallinn University of Technology, 2007.

III. Lauri Ilison and Andrus Salupere. Interactions of solitary waves in hierarchical KdV-type system. Research Report Mech 291/08, Institute of Cybernetics at Tallinn University of Technology, 2008.

Elulookirjeldus

1. Isikuandmed

Ees- ja perekonnanimi	Lauri Ilison
Sünniaeg ja -koht	26.12.1978, Tallinn
Kodakondsus	Eesti
Perekonnaseis	vabaabielus
Lapsed	2 poega (4 ja 2 aastat vanad)

2. Kontaktandmed

Aadress	Akadeemia tee 21, 12618, Tallinn
Telefon	(+372) 5 111 003
E-posti aadress	lauri@cens.ioc.ee

3. Hariduskäik

Õppeasutus (nimetus lõpetamise ajal)	Lõpetamise aasta	Haridus (eriala/kraad)
Tallinna Tehnikaülikool	2001	Tehnilise füüsika eriala / BSc
Tallinna Tehnikaülikool	2003	Tehnilise füüsika eriala / MSc

4. Keelteoskus (alg-, kesk- või kõrgtase)

Keel	Tase
Eesti keel	kõrgtase
Inglise keel	kõrgtase
Vene keel	kesktase

5. Täiendõpe

Periood	Täiendõppe läbiviija nimetus
6.–10. September 2004	CISM'i kursus: "Surface waves in Geomechanics: Direct and Inverse modelling for Soils and Rocks", Udine, Itaalia

6. Teenustuskäik

Töötamise aeg	Tööandja nimetus	Ametikoht
2001 – tänaseni	Küberneetika Instituut, Tallinn Tehnikaülikool	Insener
2000 – 2002	Sampo Pank AS	Projektijuht
2002 – 2004	Sampo Pank AS	E-panganduse juht
2004 – 2007	Sampo Pank AS	Elektrooniliste kanalite osakonna juhataja
2007 – tänaseni	Danske Bank Eesti Filiaal	Kanalite arenduse osakonna juhataja

7. Autasud

- Tallinna Tehnikaülikooli Vilistlaskogu stipendium, 1999
- Eesti Teaduste Akadeemia I auhind üliõpilaste teadustöödele, 2003

8. Sportlikud saavutused

- Eesti Noorde Meister - 16 korda allveeorienteerumine ja lestaujumine, aastatel 1993–1995
- Eesti Meister - 22 korda, allveeorienteerumine ja lestaujumine, aastatel 1994–1999
- Eesti Absoluutne Meister allveorienteeriumises 1996 ja 1998
- Eesti parim allveeorienteeruja - 1995, 1996 ja 1997
- Maailmameistrivõistlused - hõbemedal - allveeorienteerumine, Otepää, Eesti Vabariik, 1996
- Euroopa meistrivõistlused - kuldmedal - allveeorienteerumine, Seĉ, Tŝehhi Vabariik, 1997
- Maailmameistrivõistlused - pronksmedal - allveeorienteerumine, Budapest, Ungari Vabariik, 1998

9. Kaitstud lõputööd

- Waves in granular materials and dispersion analysis (Lainelevi granuleeritud materjalides ja dispersiooni analüüs), BSc, Tallinn University of Technology, 2001
- Soliton-type Waves in Granular Materials (Solitoni tüüpi lained granuleeritud materjalides), MSc, Tallinn University of Technology, 2003

10. Teadustöö põhisuunad
Mittelineaarsed lained mikrostruktuuriga materjalides (granuleeritud materjalides), solitonid

11. Teadustegevus
Teadusartiklite, konverentsiteeside, konverentsiettekannete ja teadustööde aruannete loetelu on toodud inglise keelse CV juures.